

A coupled radiogenic ($^{87}\text{Sr}/^{86}\text{Sr}$) and
stable ($\delta^{88}/^{86}\text{Sr}$) strontium isotope
approach to reconstruct past changes
in water mixing and salinity in the
Coorong Lagoon, South Australia.

Thesis submitted in accordance with the requirements of the University of
Adelaide for an Honours Degree in Environmental Geoscience

Zara Woolston
November 2020



THE UNIVERSITY
of ADELAIDE

A COUPLED RADIOGENIC ($^{87}\text{Sr}/^{86}\text{Sr}$) AND STABLE ($\delta^{88/86}\text{Sr}$) STRONTIUM ISOTOPE APPROACH TO RECONSTRUCT PAST CHANGES IN WATER MIXING AND SALINITY IN THE COORONG LAGOON, SOUTH AUSTRALIA

STRONTIUM ISOTOPE APPROACH TO RECONSTRUCT PAST CHANGES IN WATER MIXING AND SALINITY IN COORONG LAGOON

ABSTRACT

Coastal lagoons represent an interface between terrestrial and marine ecosystems that are sensitive to natural and human-induced environmental changes. The Coorong Lagoons in South Australia are part of the terminal hydrological system of the Murray Darling Basin catchment. This study explores novel geochemical analytical approaches to trace palaeo-hydrological changes in water-source mixing and to provide plausible palaeo-salinity variations within the Coorong Lagoons. Specifically using radiogenic ($^{87}\text{Sr}/^{86}\text{Sr}$) and stable ($\delta^{88/86}\text{Sr}$) strontium isotopic signatures, along with elemental ratios (such as Mg/Sr) to observe these changes by proxy. Modern and fossil carbonate archives of micro-bivalve *Arthritica Helmsi* and water chemistries of the Coorong Lagoon can provide important clues to reconstruct past hydrological changes to the system such as European settlement. Fossil water geochemical signatures are determined from fossil shells, calibrated through a comparison between modern shells and waters to infer past water characteristics such as palaeo-salinity. The acquired data and modelling suggest that there were two main sources of waters contributing to the Coorong South Lagoon; (i) seawater derived from the Southern Ocean and (ii) fresh/brackish water derived mostly from Salt Creek. Together these two water sources can explain most of the variability observed in $^{87}\text{Sr}/^{86}\text{Sr}$, $\delta^{88/86}\text{Sr}$ and Mg/Sr data in studies of carbonate shells and inferred palaeo-lagoon waters. This multi-proxy approach allowed an estimate of minimum plausible palaeo-salinity range in the Coorong South Lagoon, without the influence of carbonate precipitation and/or evaporation. The results indicate palaeo-salinities in the South Lagoon as low as 10-15 PSU (practical salinity units). Finally, results of this study also confirmed that over the last ~3275 years the waters in the Coorong South Lagoon were never 'typical' ocean waters, but rather complex mixtures of continental freshwaters with variable seawater inputs.

KEYWORDS

Strontium, Isotopes, Water Mixing, Salinity, Coorong Lagoons, *Arthritica Helmsi*

TABLE OF CONTENTS

A coupled radiogenic ($^{87}\text{Sr}/^{86}\text{Sr}$) and stable ($\delta^{88/86}\text{Sr}$) strontium isotope approach to Reconstruct past changes in water mixing and salinity in the Coorong Lagoon, South Australia	ii
Strontium isotope approach to reconstruct past changes in water mixing and salinity in Coorong Lagoon	ii
Abstract	ii
Keywords.....	ii
Table of Contents	3
List of Figures and Tables	5
1. Introduction	6
1. Background	9
2.1 Study site and geological settings	9
2.2 Palaeo-environments through <i>Arthritica Helmsi</i> carbonate proxy.....	13
2.3 Radiogenic $^{87}\text{Sr}/^{86}\text{Sr}$ and stable $\delta^{88/86}\text{Sr}$ Isotopes	14
2.3.1 Spatial variability of Sr isotopes in the Coorong Lagoon.....	16
3 Methods	18
3.1 Sample collection of modern Coorong Lagoon waters	18
3.2 Sample collection, preparation and limitations of <i>Arthritica Helmsi</i> from the Coorong Lagoons	21
3.3 Preparation and analysis of elemental concentrations.....	22
3.4 Strontium isotope analysis	23
4 Results	26
4.1 Elemental concentration data and Mg/Sr ratios	27
4.1.1 Magnesium and Strontium elemental ratios in waters	27
4.1.2 Magnesium and Strontium elemental ratios in shells	31
4.2 Radiogenic ($^{88}\text{Sr}/^{87}\text{Sr}$) and stable Strontium ($\delta^{88/86}\text{Sr}$) isotope data.....	32
4.2.1 Strontium isotope variations in waters.....	33
4.2.2 Strontium isotope variations in shells	35
4.2.2.1 Sr isotope offsets between shells and water, and impact of colour variation.....	37
4.3 Coupled multi-proxy elemental (Mg/Sr) and Sr isotope approach	40
4.3.1 Multi-proxy approach using water Data	41
4.3.2 Multi-proxy approach using shell Data	42
5 Discussion	43

5.1 Radiogenic and stable Strontium isotope variations in Coorong waters and shells: Implications for local environmental conditions	43
5.2 Impact of high versus low flow of freshwater via Salt Creek on strontium isotope composition into the South Lagoon.....	45
5.3 Variability in radiogenic and stable Sr isotope data in lagoon waters, as well as modern and fossil carbonate shells, from the Coorong Lagoons.	46
5.4 Quantifying the $\delta^{88/86}\text{Sr}$ isotope fractionation between water and shells.....	47
5.5 Assessing the effect of European settlement on the Sr isotope record of shells and palaeo-waters in the Coorong.....	47
5.6 Modelling water mixing and palaeo-salinity in Coorong South Lagoon.....	48
5.6.2 Elemental and isotope mass balance of Strontium in the Coorong Lagoon	49
5.6.2 Strontium isotope constraints on the palaeo-salinity in the Coorong South Lagoon	52
6 Conclusions	54
7 Acknowledgments	55
8 References	56
9 Appendix	60
9.1 Appendix A: Method.....	60
9.1.1 Shell classification	60
9.1.2 Radiogenic $^{87}\text{Sr}/^{86}\text{Sr}$ and stable $\delta^{88/86}\text{Sr}$ Isotopes.....	62
9.1.2.1 Preparation of sample and sample loading on rhenium filaments	62
9.1.2.2 Double-spike method and standards	63
9.1.2.3 Dynamic vs static	65
9.2 Appendix B: ICP-MS	66
9.3 Appendix C: TIMS.....	67

LIST OF FIGURES AND TABLES

Figure 1. Map of the sample area	10
Figure 2. Palaeostrandlines and facies within the Lacepede Shelf.....	12
Figure 3. Fossil <i>A.helmsi</i> from 80cm depth in core-1	13
Figure 4. A three-isotope plot ($^{87}\text{Sr}/^{86}\text{Sr}$ vs $\delta^{88/86}\text{Sr}$) with hypothesised end-member water sources in the coastal system of the Coorong Lagoons.	17
Figure 5. Sediment and water sampling	20
Figure 6. Elemental concentration of water samples against their salinity.	30
Figure 7. Elemental Mg/Sr (ppm/ppm) ratios of recent and fossil shells plotted as a function of the core depth.....	32
Figure 8. $^{87}\text{Sr}/^{86}\text{Sr}$ and $\delta^{88/86}\text{Sr}$ (‰) values for water samples taken in 2020 in Coorong Lagoon plotted together with hypothetical end-member water sources (marine, fresh and hypersaline waters)	34
Figure 9. $^{87}\text{Sr}/^{86}\text{Sr}$ and $\delta^{88/86}\text{Sr}$ (‰) data from shells with respect to core depth	36
Figure 10. $^{87}\text{Sr}/^{86}\text{Sr}$ and $\delta^{88/86}\text{Sr}$ (‰) data from shells in comparison to modern water.	38
Figure 11. $^{87}\text{Sr}/^{86}\text{Sr}$ and $\delta^{88/86}\text{Sr}$ (‰) data of modern and fossil shells plotted with respect to the 3-isotope plot.....	39
Figure 12. $^{87}\text{Sr}/^{86}\text{Sr}$ and $\delta^{88/86}\text{Sr}$ (‰) of recent waters from Coorong region, plotted against their Mg/Sr ratios.	41
Figure 13. $^{87}\text{Sr}/^{86}\text{Sr}$ and $\delta^{88/86}\text{Sr}$ (‰) of modern and fossil shells, plotted against their Mg/Sr elemental ratios.	42
Figure 14. Water flow rate in mega litres (ML) per day at the government controlled Salt Creek Regulator (SCR).	45
Figure 15. Cross-plots of $^{87}\text{Sr}/^{86}\text{Sr}$ and $\delta^{88/86}\text{Sr}$ versus Mg/Sr data in waters, based on fossil shells data with average offset of 0.122‰ for $\delta^{88/86}\text{Sr}$ applied to shells.....	51
Table 1. Standard nomenclature, their abbreviations, and the purpose/comparison that they are used for in this study.....	15
Table 2. Sr isotope results from IAPSO and JCP-1 standards from all sessions.....	25
Table 3. Overview of sample locations, dates, and names with their corresponding field measurements for modern water and shells as well as fossil shells from core 1.....	26
Table 4. Elemental concentrations in parts per million (ppm) of recent water samples.	29
Table 5. Elemental concentrations in parts per million (ppm) of shells.....	31
Table 6. Recent water $\delta^{88/86}\text{Sr}$ (‰) and $^{88}\text{Sr}/^{87}\text{Sr}$ data.....	33
Table 7. $\delta^{88/86}\text{Sr}$ (‰) and $^{88}\text{Sr}/^{87}\text{Sr}$ from modern and fossil shells from the Coorong Lagoons..	35
Table 8. Comparison of offset in $\delta^{88/86}\text{Sr}$ data between pink, white and a mixture of pink and white coloured shells.	38
Table 9. Palaeo salinity according to fraction of seawater (SW) and fraction of Salt Creek (SC) waters.	53

1. INTRODUCTION

Coastal lagoons represent the transition zone between marine and terrestrial environments. These unique coastal ecosystems provide habitat for a huge range of organisms and are important for fishing and aquaculture industries. The global degradation of these lagoon systems, (i.e. the Coorong Lagoons) has become an issue due to the overall accumulative use, sensitivity to adjustment in freshwater and seawater flow rate, and increasing evaporation and water loss due to climate change (Phillis et al., 2011). Human-induced salinisation of lagoons is commonly observed in the palaeo-data and historical records, illustrating the influence anthropogenic water manipulation has on the lagoon environment (Saunders et al., 2007). In Australia, water flow dependent coastal systems, such as the Coorong Lagoons, are strongly affected by upstream water flow allocation and intermittent rainfall (Webster & Harris, 2004). The River Murray is the principal river in the Murray Darling Basin (MDB) and travels through three states of Australia. It terminates in South Australia in the Coorong Lagoon, Lower Lakes (Alexandrina and Albert) and the Murray Mouth (CLLMM) all considered designated Ramsar sites (Kingsford et al., 2011). In the Coorong Lagoon salinity largely depends on water mixing between fresh/brackish waters and seawaters from various inputs (Shao et al., Submitted). Palaeo water mixing can be observed through changes preserved within bio and geochemical proxies as tracers of environmental characteristic in fossils, such as the bivalve *Arthritica Helmsi* used in this thesis, with some challenges (Andrews et al., 2016; Chamberlayne et al., 2019; Farkaš et al., 2007; Gillanders & Munro, 2012; Phillis et al., 2011; Schöne et al., 2010). Past use of *A. helmsi* as an isotopic environmental tracer by Chamberlayne et al. (2019) showed no differentiation between shell colour variation and thus separation of the two variants (pink and white)

was undertaken to observe if there was a biochemical ratio difference (James & Bone, 2011). Three isotopes of strontium are used in this study; ^{88}Sr , ^{87}Sr and ^{86}Sr . Radiogenic ($^{87}\text{Sr}/^{86}\text{Sr}$) strontium has a long residence time within the global ocean budget and its isotopic signature is stable, an increase of water content contributed by continental waters such as rivers increases ^{87}Sr due to radioactive decay of ^{87}Rb originating from continental weathering (Capo et al., 1998; Hodell et al., 1990; Kober et al., 2007; McArthur et al., 2001). Combining this marine constant together with mixing of continental waters allow $^{87}\text{Sr}/^{86}\text{Sr}$ to act as a tracer of water sources. Stable strontium ($\delta^{88/86}\text{Sr}$) can be used to trace and act as a proxy for physical characteristics within aquatic systems such as temperature shown by Fietzke and Eisenhauer (2006) and also by Fruchter et al. (2016). Within the Coorong Lagoon these isotopic tracers can be used to observe water mixing and salinity, grouping water source inputs and creating end-members. There are three distinct isotopically different end-members within the Coorong Lagoon; freshwater, marine and hypersaline (Andrews et al., 2016; McArthur et al., 2001; Shao et al., Submitted; Vollstaedt et al., 2014).

The main aim of this project is to use coupled radiogenic and stable Sr isotope tracers to infer past water mixing and salinity changes in the Coorong Lagoon, before and after European settlement. Using analysis of $^{87}\text{Sr}/^{86}\text{Sr}$ and $\delta^{88/86}\text{Sr}$ in fossil shells recovered from a sediment core from the Coorong Lagoon, together with a calibration of the above isotope tracers in present-day lagoon and recent shells. This data will then be plotted in a three-isotope plot ($^{87}\text{Sr}/^{86}\text{Sr}$ vs $\delta^{88/86}\text{Sr}$) to test the plausibility of hypothesised palaeo-salinity scenarios for the Coorong Lagoon before European settlement, including (i) fresh/brackish, (ii) marine, and/or (iii) hypersaline waters. This thesis focuses on the

ability of Sr geochemical analysis to model water mixing and salinity as the CLLMM is listed with the Ramsar convention on wetlands of international importance. This convention has been put in place to stop wetland destruction globally and encourages correct management and conservation of what is left (Kingsford et al., 2011).

This study uses a collection of recent waters, modern *A. helmsi* shells and fossil *A. helmsi* shells from the Coorong Lagoon for analysis through ICP-MS and TIMS. Elemental concentrations were analysed through ICP-MS and radiogenic ($^{87}\text{Sr}/^{86}\text{Sr}$) and stable ($\delta^{88/86}\text{Sr}$) strontium was analysed through TIMS. Combining the above techniques this study aims to (i) Use Sr isotopes as a proxy for local water chemistry and salinity conditions to determine the effect of changes in seasonal water output, sources, and flow on isotopic signatures, (ii) Assess the variability of radiogenic and stable Sr isotope ratios in lagoon waters as well as past and present *A. helmsi* carbonate shells and (iii) Compare modern day and pre-European settlement *A. helmsi* carbonate shells' radiogenic and stable strontium signatures to determine potential historical changes in water source and salinity in the South Lagoon. This Sr-isotope based proxy information provides a model for water source mixing in the South Lagoon over the past 3275 years (dated via ^{14}C technique by Foster, et al. pers. comm. 2020) by comparing $^{87}\text{Sr}/^{86}\text{Sr}$ ratios and $\delta^{88/86}\text{Sr}$ against Mg/Sr elemental ratios in modern and fossil shells. From this model inferred minimum palaeo-salinity of the South Lagoon can be theorised. This information can then be used to implement better strategies of conservation tailored to the dynamics of the Coorong Lagoons.

1. BACKGROUND

2.1 Study site and geological settings

The Coorong consists of two lagoons (North and South), they join at the Coorong's narrowest near Parnka Point see Figure 1. In times of low river flow and high evaporation, generally in summer or during the dry seasons, the water level drops, and these two lagoons can become separate water bodies with a minimum or very restricted exchange of waters. A salinity gradient with increasing salinity from South to North exists across the Coorong, this is dependent on freshwater influx. Whilst both North and South Lagoons fluctuate in their salinity levels, the South Lagoon tends to remain more saline and has now been classified as permanently hypersaline (Brookes et al., 2009; Reeves et al., 2014; Shao et al., 2018). For this study hypersaline is considered to be >70 PSU, seawater is 30-35 PSU and freshwater is <15 PSU (Brookes et al., 2009). The salinity of the South Lagoon commonly exceeds 100 PSU (Practical Salinity Unit) during summer or dry seasons (February and March) and drops to ~80 PSU or lower during winter or wet seasons (July). European settlement within the MDB and the CLLMM has brought about the regulation of water flow, such as the Tauwitechere barrages built ~1930 (seen in red in Figure 1) (Lower et al., 2013; Mosley et al., 2018; Reeves et al., 2014). This has led to decreased water flow and, in combination with increased evaporation during summers, has led to the South Lagoons hypersaline classification.

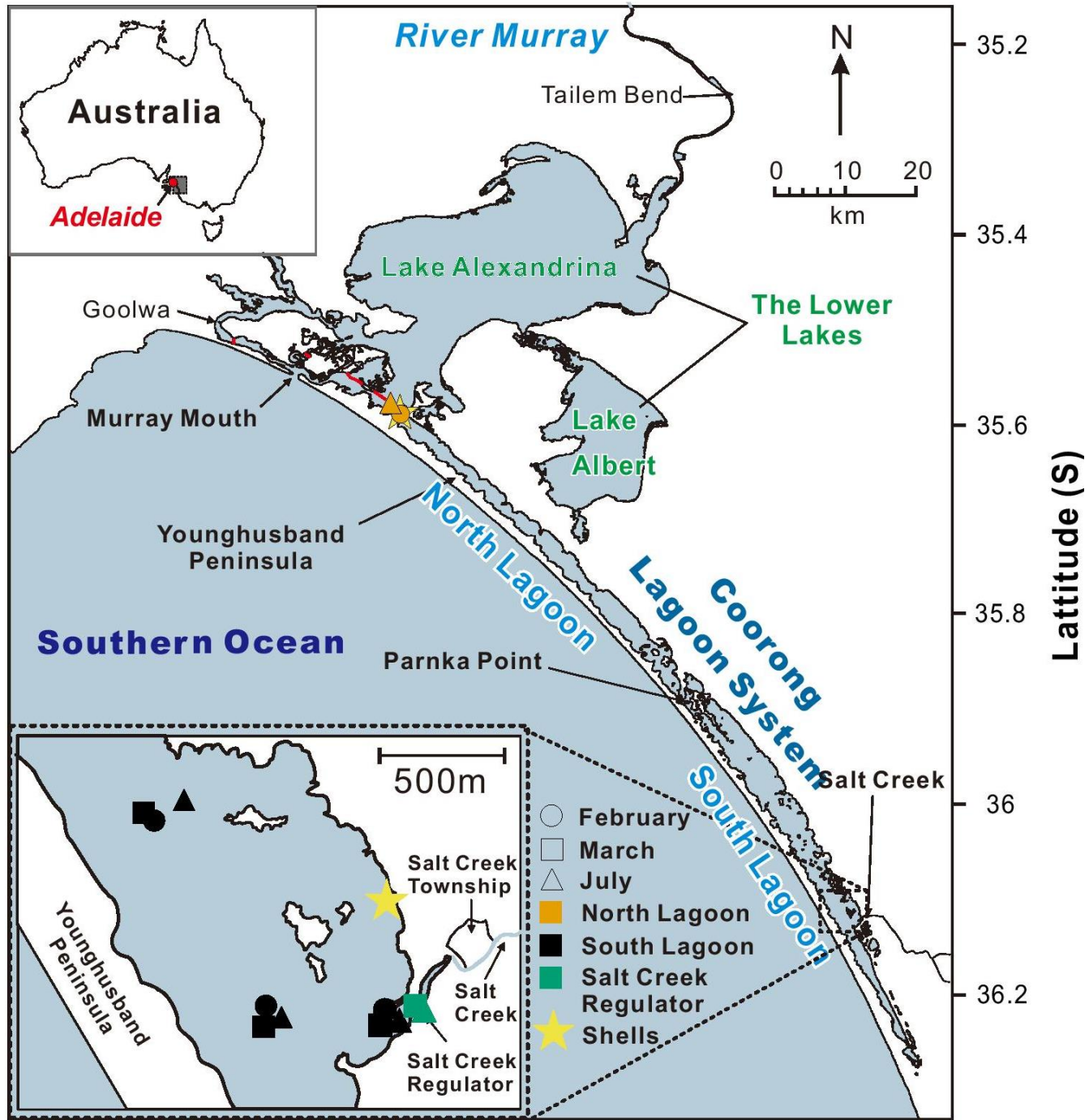


Figure 1. Map of the sample area modified from Shao et al. (Submitted) showing waters and shells that were sampled during 2020 and a core (core-1) sampled in 2019. The red lines show Tauwichee barrages, specific locations and field measurements can be seen in Table 3.

Salinity plays a role in species biodiversity and abundance, hyper-salinity in the Coorong has contributed towards a modern decline in diversity of waterbirds, fish and

diatoms (Brookes et al., 2009; Haynes et al., 2011; Phillips & Muller, 2006). As well as a decrease in certain fossil species that are saline sensitive over the last ca. 1000 years (Reeves et al., 2014) and a drastic change in biomarkers within sediments suggesting an increase in salinity correlating with European settlement and an increase in droughts (Tulipani et al., 2014). Water mixing phenomena between different water sources within the CLLMM affects geochemistry and isotope composition of local waters, the latter is linked to seasonal flow rate change, multiple water source mixing, historical changes in water flows and degrees of evaporation (Phillis et al., 2011; Shao et al., 2018). Due to its very nature the more restricted South Lagoon is expected to have distinctive Sr isotope ratios that seasonally vary but group around the isotopic end-member tied to hyper-salinity. These end-members will provide the basis of using Sr as a proxy to distinguish palaeo-salinity, see Figure 4 (Shao et al., 2018). If the South Lagoon was ever historically dominated by seawater input, then the fossil shells will have a radiogenic and stable strontium isotopic signature that record this. Seawater from the Southern Ocean is noticeably different, in radiogenic Sr, to hypersaline, or fresh/brackish waters from groundwater aquifers and Salt Creek (Shao et al., 2018). Using radiogenic and stable Sr isotopes it is possible to differentiate between seawater, hypersaline and freshwater signatures, due to residence time, evaporative controlled carbonate precipitation and continental weathering, respectively.

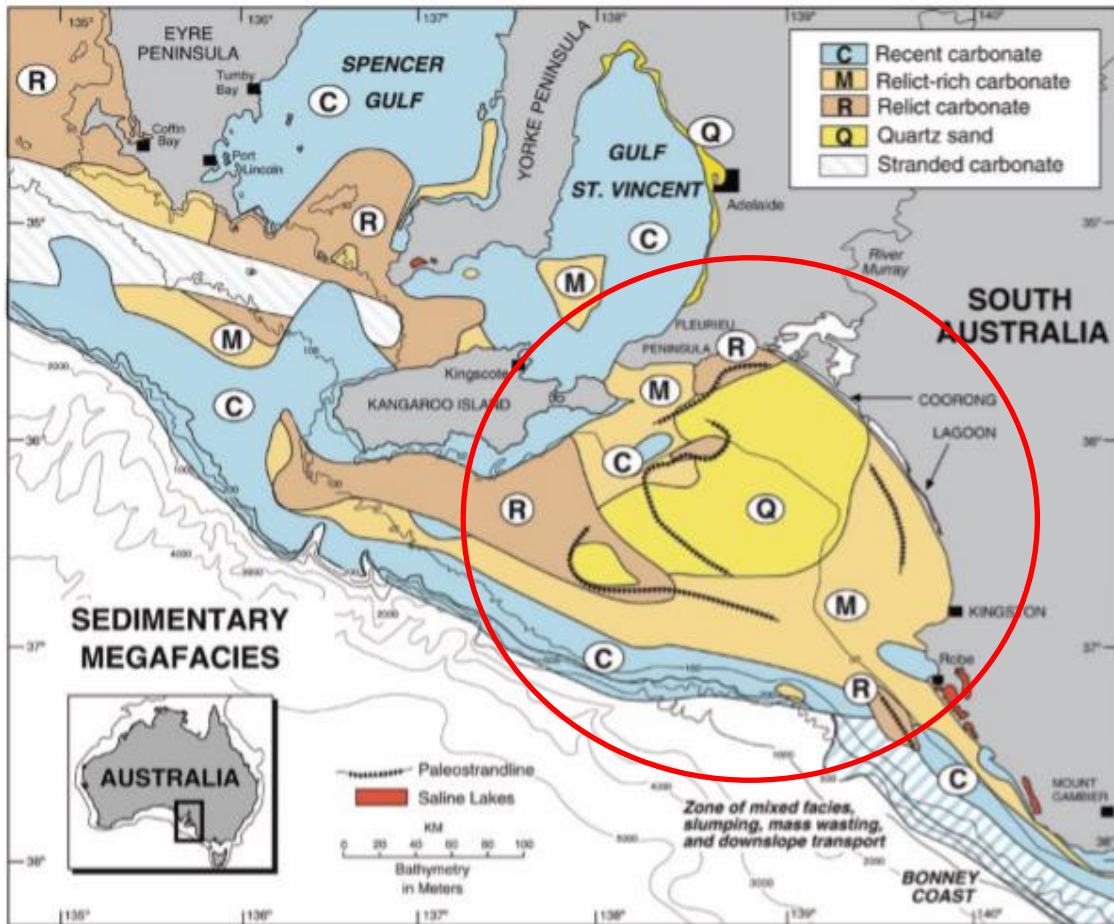


Figure 2. Palaeostrandlines and facies within the Lacedpede Shelf (shown within the red circle), Southwest of the Coorong modified from James and Bone (2011).

The morphology and depositional environment of the Coorong Lagoon system has been shaped by glacial lowstands (regression) and highstands (transgression). The changes in water levels along the coast are preserved in the sedimentary facies in the Lacedpede Shelf Southwest of the Coorong. As illustrated in Figure 2 the northern section of the Coorong is developed on calcareous quartz sand whereas in the South there is a palaeostrandline southeast of the coast that contains relict-rich molluscan sand (James & Bone, 2011). The Coorong water body has been formed between the last interglacial shoreline, when sea levels were higher, and the modern sand dunes of the Young

Husband peninsula that occurred in the late Holocene as sea levels lowered (Mosley et al., 2018).

2.2 Palaeo-environments through *Arthritica Helmsi* carbonate proxy

The Coorong represents a natural temporal and spatial variability in ecosystem characteristics. McKirdy et al. (2010) used isotope tracers such as carbon and nitrogen in biota and sediment to observe biogeochemical evolution from mid to late Holocene showing an in steady increase in salinity from ~540 B.P. in the Coorong. Species of foraminifera, ostracods and molluscs have been used by Lower et al. (2013) to assess species change as a proxy for salinity, drought and deposition environment with respect to the first appearance of *Pinus* pollen as a European settlement proxy.

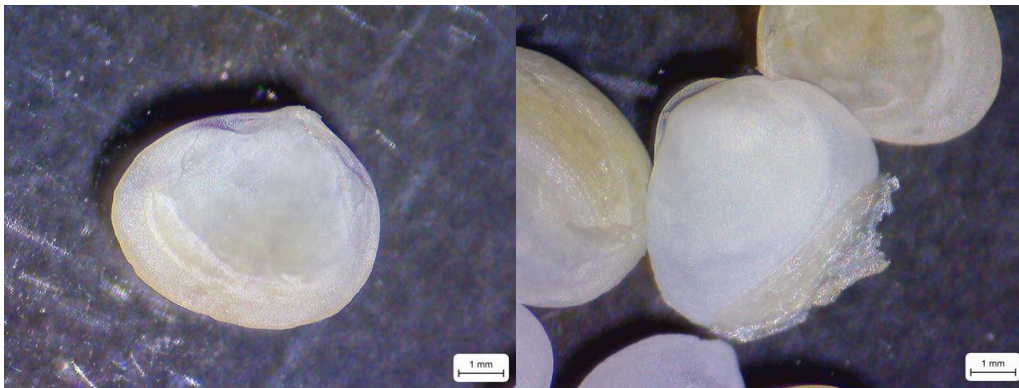


Figure 3. Fossil *A. helmsi* from 80cm depth in core-1 separated from sediment and methodically cleaned, specific location available in Table 3. Classified as pink (left) classified as white (right), with some of the periostracum showing as the fibrous sheet still attached.

A. helmsi is a small bivalve (Figure 3), that is common in the South-east of South Australia, the Coorong Lagoon system included. Chamberlayne et al. (2019) found that fossil shells of *A. helmsi* could be used as a tracer but if water characteristics such as ambient isotopic water signatures and salinity were unconstrained tracing environmental trends should be done with caution. Shao et al. (Submitted) built on this information through observing a comparison between modern *A. helmsi* shells with local water and

generally found that as stable Sr ($\delta^{88/86}\text{Sr}$) increased so did salinity. In previous studies by Chamberlayne et al. (2019), Shao et al. (2018) and Shao et al. (Submitted) distinguishing between colouration (white vs pinkish) of *A. helmsi* carbonate shells has not been discussed in any detail. Separating these individuals with respect to colouration into 'in-situ' (i.e. pinkish) and 'redeposited' (white/bleached) shells could have some impact on measured Sr concentrations. This could be due to carbonate shells being transported or redeposited to this location through water movement or ingestion by predators. Analysis of shells without colour separation could misconstrue shells taken potentially from both another site and a different time period than that in question (James & Bone, 2011). Reconstructing past salinity and water mixing from fossil studies of the carbonate aragonitic shell of *A. helmsi* in the Coorong can provide information to improve management of the CLLMM. (Chamberlayne et al., 2019; Lower et al., 2013; Reeves et al., 2014).

2.3 Radiogenic $^{87}\text{Sr}/^{86}\text{Sr}$ and stable $\delta^{88/86}\text{Sr}$ Isotopes

Strontium has four naturally occurring isotopes, with the following percent abundances: ^{84}Sr : 0.56%, ^{86}Sr : 9.87%, ^{87}Sr :7.04% and ^{88}Sr :82.53%. Radiogenic ^{87}Sr isotopes represent the product of radioactive decay of ^{87}Rb with a half-life of ~48.8 billion years (Capo et al., 1998). Radiogenic Sr isotopes ($^{87}\text{Sr}/^{86}\text{Sr}$) can be used in the Coorong Lagoon and wider CLLMM system because the local geology and bedrock are relatively old when observing the Sr marine budget (Bourman & Barnett, 1995; Krabbenhöft et al., 2010). The radiogenic Sr isotope signature of present-day seawater of 0.70917, is globally homogeneous as a result of the long residence time (~2.5 million years, Myr) of ^{87}Sr in modern oceans (Hodell et al., 1990; Vollstaedt et al., 2014). Radiogenic

strontium ($^{87}\text{Sr}/^{86}\text{Sr}$) can be used in coastal environments with reasonable success due to the above contrast in $^{87}\text{Sr}/^{86}\text{Sr}$ signature of marine (~ 0.70917) versus continental (> 0.7110) waters (see Krabbenhöft et al., 2010; McArthur et al., 2001; Vollstaedt et al., 2014). The method for determining stable strontium ($\delta^{88/86}\text{Sr}$) value or variation in mass-dependent Sr isotope effects on $^{88}\text{Sr}/^{86}\text{Sr}$ ratios (see also Equation 1 below) has evolved over last ca. 15 years. With pioneering studies using MC-ICP-MS (Multicollector-Inductively Coupled Plasma-Mass Spectrometry) instruments coupled with a ‘sample to standard’ bracketing approach (Fietzke & Eisenhauer, 2006) to more robust and precise approaches, used in this study, that rely on TIMS and double spike techniques (Krabbenhöft et al., 2009).

Table 1. Standard nomenclature, their abbreviations, and the purpose/comparison that they are used for in this study.

Abbreviation	Abbreviation expanded	Purpose/Comparison
NIST SRM 987	National Institute of Standards and Technology Standard Reference Material 987	Widely used Sr concentration to compare accuracy of my results (strontium carbonate SrCO_3 isotope reference material)
IAPSO	International Association for the Physical Science of the Oceans	Seawater comparison to my saline waters
JCp-1	Japan Coral <i>Porites</i> sp.	Biogenic carbonate (CaCO_3) comparison to fossil and modern <i>A. helmsi</i>

Note that all stable Sr isotope data presented in this thesis are expressed as ‘delta’ values ($\delta^{88/86}\text{Sr}$), in per mil (‰) relative to the standard NIST SRM 987 (see Table 1 for more details) calculated as show below:

Equation 1

$$\delta^{88/86}\text{Sr} = \left[\frac{(^{88}\text{Sr}/^{86}\text{Sr})_{\text{sample}}}{(^{88}\text{Sr}/^{86}\text{Sr})_{\text{NIST SRM 987}}} - 1 \right] \times 1000$$

The $\delta^{88/86}\text{Sr}$ data presented in this thesis are normalised following Equation 1 further details available in Appendix C. For more details on the TIMS and double-spiking method that was used also in this study for determining $\delta^{88/86}\text{Sr}$ variations in waters and carbonates please see Appendix A. Besides SRM 987, the other two internationally recognised standards (i) IAPSO and (ii) JcP-1 have been used and analysed in this study (for details see also Table 1 and Table 2).

2.3.1 SPATIAL VARIABILITY OF SR ISOTOPES IN THE COORONG LAGOON

Generally there are three types of main water input into the Coorong Lagoons, including (i) seawater from the Southern Ocean, (ii) freshwater via Murray River through the Lower Lakes and (iii) brackish water from the local ground water travelling through the porous bedrock limestone and/or supplied via Salt Creek input (Shao et al., 2018; Shao et al., Submitted). The relationship between radiogenic $^{87}\text{Sr}/^{86}\text{Sr}$ and stable $\delta^{88/86}\text{Sr}$ data can be used as a powerful tracer to differentiate among different Sr sources (and through inference water sources) in hydrological and geological systems (Krabbenhöft et al., 2010). The complex nature of water exchange and mixing at a marine-continent interface, such as the Coorong Lagoon and CLLMM system, might be clarified via the 3-isotope approach based on $^{87}\text{Sr}/^{86}\text{Sr}$ vs $\delta^{88/86}\text{Sr}$ cross-plot in both modern and palaeo hydrological systems (see Shao et al., Submitted; and Figure 4).

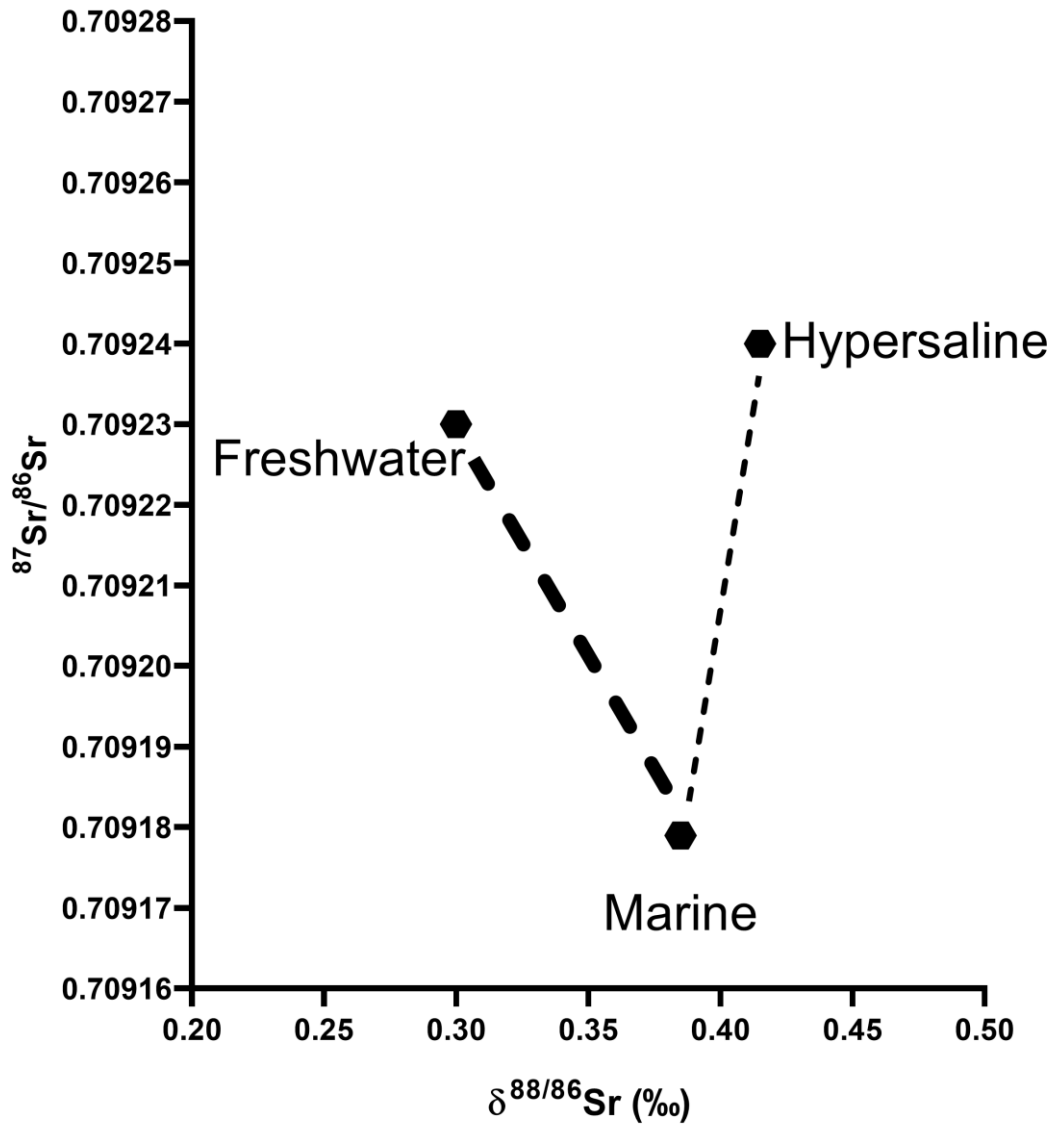


Figure 4. A three-isotope plot ($^{87}\text{Sr}/^{86}\text{Sr}$ vs $\delta^{88/86}\text{Sr}$) with hypothesised end-member water sources in the coastal system of the Coorong Lagoons. The marine end-member is represented by data from IAPSO (n=3) standards; and compositions of local freshwater and hypersaline lagoon waters have been adopted from Shao et al. (Submitted); and these end-members will be referred to throughout the thesis.

Main Sr isotopic end-members or plausible water source are illustrated in Figure 4; however the isotope composition of some of these sources (e.g. continental waters and/or groundwater) can also change seasonally depending on the input (flow rate) and output (evaporation) within the system (Shao et al., 2018). Typical seawater radiogenic

isotope signatures are expected to be homogeneous throughout the year and last millennia due to the long residence time of Sr in seawater. Importantly the radiogenic signature $^{87}\text{Sr}/^{86}\text{Sr}$ of local lagoon waters is directly imparted on the Sr isotope composition of precipitated carbonates and /or shells (without isotope fractionation or offsets), thus providing a direct tracer of water source mixing and Sr provenance (Shao et al., 2018). Carbonate formation preferentially incorporates lighter ^{86}Sr into precipitates (relative to solution or water), due to mass-dependent and biological isotope effects. Salinity varies as a gradient in the lagoon and the concentration of salinity can affect carbonate precipitation, which can then cause stable strontium enrichment within carbonates (Shalev et al., 2017; Shao et al., Submitted; Singurindy et al., 2004). This causes a typical ‘offset’ that has been found to be approximately 0.1‰ to 0.2‰ lighter in the shells comparing to ambient waters (Shao et al., Submitted; Vollstaedt et al., 2014).

3 METHODS

During 2020 a total of 27 samples of waters ($n = 13$) and shells ($n = 14$) were taken from the Coorong Lagoon, majority of samples were taken from the South Lagoon with two water samples and one shell sample taken from the North Lagoon. This is a part of the ongoing research related to a greater Project Coorong and its Healthy Coorong Healthy Basin (HCHB) initiative.

3.1 Sample collection of modern Coorong Lagoon waters

Three water samples were taken in February-2020, five in March-2020, and an additional five were taken in July-2020. In the March sampling trip, a sample of modern

carbonate shells of *A. helmsi* was also taken from the North Lagoon. Water samples were taken from the surface of the water from the edge of a commercial fishing boat (exact locations and coordinates are listed in Table 3). All samples were kept below 4°C in a cool box and after collection in a cold store and filtered through a 0.45µm cellulose nitrate membrane filter either in the field or the day after (see Figure 5A and 5B). All samples should have been acidified after filtration, but February and March water samples were not due to human error. Water quality measurements including pH and Salinity were taken at each location using an YSI Pro Series portable probe, and results are listed in Table 3. All water samples were collected in pre-cleaned HDPE plastic bottles that were acid cleaned with ~6M HCl overnight at 90°C and then rinsed with DI (deionised) water to be contaminant-free.

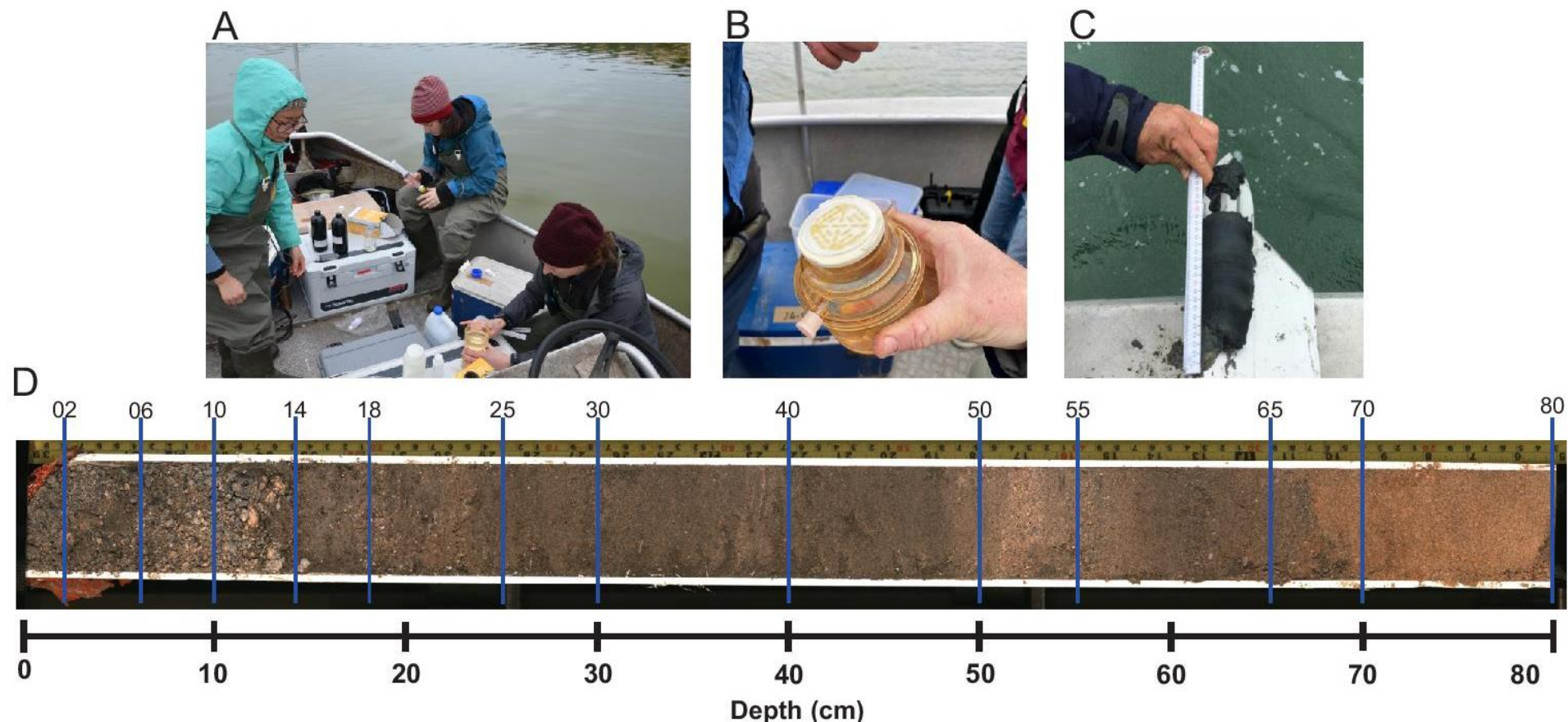


Figure 5. (A) In field filtration of modern water samples with a 0.45 μ m filter fitted on a syringe as well as a hand pump filtering device also seen in (B) with a 0.45 μ m cellulose nitrate filter attached, the darker material is local biota such as algae that has been filtered out from the water sample captured in the bottom of the pump (C) A top sediment sample taken at site COOR 50 in North Lagoon where the modern *A. helmsi* samples were observed and extracted from the first 10cm of sediment (exact location in Table 3). (D) Core-1 taken from the South Lagoon, full details in Table 3. Blue lines indicate where a 1cm thick ‘bulk sediment’ was taken and fossil shells were processed from these bulk sediments. Sample names in Table 6 correspond to label names on blue lines above. Initially horizons were evenly spread across the core, but some horizons were completely devoid of shells and thus not included in this study

3.2 Sample collection, preparation and limitations of *Arthritica Helmsi* from the Coorong Lagoons

In this study, a sediment core (80cm long and 75mm wide) containing *A. helmsi* fossils (Figure 5D) was collected from the South Coorong Lagoon. The sediment core was ^{14}C dated at the Australian Nuclear Science and Technology Organisation (ANSTO, Lucas Heights, Sydney) at each horizon. Unfortunately, due to the high carbonate content at this site, there was not enough ^{14}C left to complete dating at all horizons. This resulted in only one date record for the whole core which was at ~80cm, yielding an age of 3275 \pm 25 B.P (Foster, et al. pers. comm. 2020). From the sediment core-1, collected from the South Lagoon (see Figure 1) in June 2019, a total of 13 individual horizons across the core were selected with regards to shell availability.

In addition to this, modern *A. helmsi* were sampled from the sediment surface in Tauwitchere with a telescopic corer (North Lagoon, see Figure 1 for location and Figure 6C for image of modern sediment). Modern shells were ascertained to be alive as they were articulated, and the organism was found inside upon cleaning. This sediment sample was stored below 4°C and was then freeze dried at a later date in a SCANVC Coolsafe 55-9 overnight at -52°C. Water and shell samples were simultaneously collected to enable comparison between modern shell and present-day lagoon water. Present-day water and modern shell samples could not be collected directly at the site from which the studied core originated (see Figure 1). As the current water samples were taken during a low flow period at the end of summer when the location of the core site was completely dry and exposed above water level. Additionally, due to the hypersaline nature of the South Lagoon waters where the core was sampled, the

environment is unsuitable for shell organisms, including *A.helmsi*, to survive in the lagoon.

Collected shells were then washed in DI water and further cleaned with a small brush to remove majority of attached sediment material. The shells were then submerged in 10% H₂O₂ for 3 days (to oxidise organic material), and then a very mild (0.27M) HCl acid was applied to dissolve outer organic surfaces (e.g. periostracum) from the carbonate shells. Some shells still had light-coloured sediment attached on the inside of the shell, and as these shells were too delicate and small for the sediment to be physically removed, these shells with attached sediment were removed from the group to eliminate sediment contamination after total shell dissolution. Shells were then inspected and separated according to their colour, to provide a comparison between white and pink coloured shells. The distinction between the colours of shells is as follows (images in Appendix A): any pink colouration that remained on the shell meant they were counted as pink and shells that were completely white or bleached were classified as white shells (James & Bone, 2011).

3.3 Preparation and analysis of elemental concentrations

All water and shell samples were acid digested, then diluted using 2% HNO₃ (as described below) for the purposes of ICP-MS analysis at Adelaide Microscopy, using an Agilent 8900 instrument. To measure concentrations of selected elements, including Sr and Mg. For this purpose, all samples were diluted into 5ml acid-cleaned plastic vials (cleaned in 6M HCl overnight). For all waters dilution factors were calculated based on their salinity (PSU) measured in the field by the probe (see Table 3), to attain optimal signals and intensities for ICP-MS analysis of the elements of interest. Cleaned shell of

A. helmsi were weighed using a 6-digit balance Meettler Toledo weights recorded and afterwards the shells were dissolved in 3ml of ultra-pure 0.5M HCl in Teflon vials, followed by evaporation of sample solutions at 90°C on a hot plate overnight. The evaporated residue (from acid digested shells) was then re-dissolved in 2% HNO₃ applying a dilution factor of 1000 (to prepare stock sample solutions), calculated based on specific shell weight before dissolution. In addition prior to ICP-MS analysis a further dilution factor of 10 (using 2% HNO₃) was applied to meet desirable Sr concentration range ideal for the instrument sensitivity and specific calibration thresholds.

3.4 Strontium isotope analysis

Water samples collected in February and March, 2020 were based on field measurements of salinities and the linear relationship (Equation 2), between Sr concentration (ppm) and salinity (PSU) of waters from previous studies (Gillanders & Munro, 2012; Shao et al., Submitted). July samples were calculated according to measured elemental concentrations.

Equation 2 (Shao et al., Submitted)

$$Sr \text{ (ppm)} = 0.2251 * Salinity \text{ (PSU)} + 0.4597$$

For the isotope analysis on TIMS, an aliquot of sample containing 500ng of Sr was pipetted into Teflon vials that were cleaned over a period of approximately a week. Specifically 48 hours on a hotplate at 140 °C in 6M HNO₃ rinsed with DI (deionised) water and submerged in 6M HCl at 140 °C for 48 hours another DI rinse and then dried. Column chemistry was carried out following the Sr SPS Micro Bin Spin column procedure and procedural blanks returned, on average, 14 pg Sr (\pm 8.54), (n=3). This is

considered appropriate procedural blank for Sr isotope analysis accounting for less than 0.1% of Sr loaded (Krabbenhöft et al., 2009; Vollstaedt et al., 2014). Column chemistry purified samples of Sr were then loaded onto successfully outgassed rhenium filaments using no more than 2.3 Amps of electrical current run through G^w INSTEK programmable power supply (see Appendix A for further method). Once samples are securely loaded on the filament, the filaments are then fastened to a TIMS turret using the bracketing procedure outlined in appendix A.

In this thesis different TIMS analytical approaches were used for determination of radiogenic $^{87}\text{Sr}/^{86}\text{Sr}$ ratios, and stable Sr isotope variations; and these approaches are described in more detail in Appendix A. A summary statement of the accuracy and precision of the data presented through use of these analytical technique follows in Table 2. All sessions carried out in this study resulted in the average ‘sample to spike’ ratio using double-spike DS3 of around 20.5631 (± 4.5948) for all samples analysed, (n=35), thus within the range of optimal spiking conditions for our setup. Table 2 below displays average radiogenic and stable strontium for well-known and used IAPSO and JCP-1 compared to NIST SRM 987 standards. These standards are bracketed around field samples (see Appendix A for example of bracketing procedure) to apply normalisation for long term and short-term drift (see Appendix C for normalisation of standards). All radiogenic and stable strontium data displayed in this thesis is normalised appropriately according to the method by Krabbenhöft et al. (2009).

Table 2. Sr isotope results from IAPSO and JCP-1 standards from all sessions, including radiogenic and stable Sr isotope data, along with published values on standards for a comparison. Highlighted are average $\delta^{88/86}\text{Sr}$ and $^{87}\text{Sr}/^{86}\text{Sr}$ data from this study, with accompanied standard deviation (SD) and standard error (SE).

Standard	Session	Date	$\delta^{88/86}\text{Sr}$ (‰)	2*SE	$^{87}\text{Sr}/^{86}\text{Sr}$	2*SE	$^{84}\text{Sr}_{\text{sp}}/^{84}\text{Sr}_{\text{rsa}}$
IAPSO	1	April 2020	0.384	0.012	0.709183	0.000003	24.37
	2	June 2020	0.408	0.013	0.709179	0.000004	21.92
	3	August 2020	0.363	0.012	0.709176	0.000003	23.13
	Average		0.385	0.013	0.709179	0.000003	23.14
	SD		0.023		0.000004		1.23
	<i>Published values</i>	<i>Krabbenhoft et al. 2009</i>	0.387		0.709169	0.000007 (n=10)	
		<i>Andrews et al. 2016</i>	0.396	0.005 (n=54)	0.709180		
JCP-1	4	August 2020	0.223	0.013	0.709183	0.000003	20.67
	5	August 2020	0.223	0.012	0.709170	0.000004	21.09
	6	September 2020	0.212	0.014	0.709176	0.000262	20.66
	Average		0.219	0.013	0.709176	0.000090	20.81
	SD		0.006		0.000007		0.24
	<i>Published values*</i>	<i>Vollstaedt et al. 2013</i>	0.193	0.004 (n=32)	0.709172	0.000004	
		<i>Krabbenhoft et al. 2009</i>	0.197	0.015 (n=8)	0.709164	0.000001 (n=3)	

$^{84}\text{Sr}_{\text{sp}}/^{84}\text{Sr}_{\text{rsa}}$ (or sample to spike ratio) represents a ratio of ^{84}Sr in the spike in relation to the amount of ^{84}Sr in the sample.

*Published values for JCP-1 can be variable and are not widely accessible (Weber et al., 2018).

4 RESULTS

The results of this study, including field measurements, and coupled $^{87}\text{Sr}/^{86}\text{Sr}$ and $\delta^{88/86}\text{Sr}$ and elemental concentration data are summarised in the sections below. These include results from waters, as well as modern and fossil shells.

Table 3. Overview of sample locations, dates, and names with their corresponding field measurements for modern water and shells as well as fossil shells from core 1.

Date Collected	Relative location	Latitude (degrees South)	Longitude (degrees East)	Sample Name	Temp (°C)	Salinity (PSU)	pH
13/02/2020	SC Mouth	36.133	139.637	LZ1	22.2	99	7.79
13/02/2020	1.8km West SC	36.132	139.620	LZ3	21.7	99.34	8.06
13/02/2020	NW Snipe Island	36.110	139.604	LZ5	22.1	99.21	8.09
11/03/2020	South SC	36.134	139.637	COOR 01	18.7	103.88	7.51
11/03/2020	1.8km West SC	36.134	139.620	COOR 04	18.7	104.55	7.94
11/03/2020	Snipe Point	36.109	139.608	COOR 07	19.2	104.89	8.09
13/03/2020	Tauwitchere*	35.598	139.024	COOR 50	19.9	31.5	8.3
12/03/2020	SC Fish way	36.132	139.642	SCR	22.5	14.95	11
6/07/2020	SC Outlet	36.134	139.634	N9	11.3	83.16	7.86
6/07/2020	1.8km West SC	36.126	139.635	S7	11.5	84.25	7.84
6/07/2020	Snipe Point	36.110	139.604	S6	11.3	83.84	7.95
7/07/2020	Tauwitchere	35.590	139.016	N5	--	29.42	--
6/07/2020	SC Fish way	36.132	139.642	SCR(2)	11.3	9.99	8.95
14/06/2019	Core 1	36.119	139.638	Core 1	N/A	N/A	N/A

* Site where the modern shell samples were taken. Salinity PSU is salinity in practical salinity units. SC represents Salt Creek and SCR is Salt Creek Regulator.

During the sampling period, the salinity of waters in the South Lagoon ranged from ~83 PSU in winter and reached over ~100 PSU in the summer months (see Table 3). In contrast, the North Lagoon waters were less saline than the South Lagoon (Brookes et al., 2009; Reeves et al., 2014), with a typical salinity for North Lagoon of ~30 PSU, close to normal seawater. The waters sampled from Salt Creek Regulator (SCR) were generally fresh to brackish with salinities ~10 PSU (Table 3).

4.1 Elemental concentration data and Mg/Sr ratios

Strontium concentration in all samples is required to (i) properly spike a sample with an optimal amount of Sr isotope double-spike, and (ii) to load enough Sr for high-precision stable and radiogenic Sr isotope analysis by TIMS. In addition, elemental concentration data, and specifically elemental ratios such as Mg/Sr, can be used as additional and complimentary palaeo-environment tracer in conjunction with stable and radiogenic Sr isotopes. The sections below present such elemental ratio of Mg/Sr data measured in both waters and shells, where the concentrations of Sr and Mg in studied waters show a strong positive a linear correlation with the salinity of waters (see Figure 6; and see also Gillanders & Munro, 2012).

4.1.1 MAGNESIUM AND STRONTIUM ELEMENTAL RATIOS IN WATERS

Water samples analysed in this study generally showed expected elemental chemistry for the months waters were sampled in. COOR-50 sampled in the North Lagoon sampled during summer (March), see Table 3, is a mixture of seawater from the Southern Ocean through the Murray Mouth, with the fresh/brackish water of the Lower Lakes. Sample N5 is also from the water mixing zone of the North Lagoon but during winter (July), the elemental chemistry between these two similar locals differ seasonally and potentially in their preparation method. Exceptions to expected elemental chemistry originate from two potential error sources as machine error was eliminated through calibration with known solutions (see Appendix B): (i) inconsistent acidification of waters and (ii) inconsistent dilution of waters. Strontium is a non-conservative element that follows Ca in biogeochemical cycles, and it can precipitate out of the solution to form aragonite or calcite along with Ca, aragonite in the case of *A.helmsi*. Before

storage and analysis acidification of water samples is required to prevent formation of CaCO_3 minerals in sampled waters, which might impact measured Sr concentration and eventually also Sr isotopes. Accordingly if waters are not acidified then the sample might yield lower than expected Sr concentrations due to secondary precipitation of carbonate minerals during storage. Due to omission during initial stages of the project, only July water samples were acidified but not February and March before analysis. Thus the observed spread in Sr concentration data in water samples (Table 3) collected in February and March compared to July samples, and their non-ideal correlation with salinity, might suggest that concentration data from this sampling period could be affected by such secondary processes linked to carbonate precipitation during sample storage or dilution calculation error. Therefore, these results might not be robust and need to be taken with caution. Note however, that these effects will not impact data measured in shells, as the latter are directly acid digested and processed.

Table 4. Elemental concentrations in parts per million (ppm) of recent water samples taken in February, March and July in 2020 and have been back calculated from ICP-MS diluted concentrations with respect to salinity concentrations (see Appendix B for more detailed back calculations).

Date	Salinity (PSU)	Mg (ppm)	Sr (ppm)	Mg/Sr (ppm/ppm)	
February	LZ 1	99	5587.84	37.38	149.48
	LZ 3	99.34	3354.75	22.19	151.19
	LZ 5	99.21	3289.39	19.22	171.18
March	COOR - 01	103.88	3847.84	22.20	173.36
	COOR - 04	104.55	2995.48	17.58	170.43
	COOR - 07	104.89	7844.90	51.71	151.72
	COOR - 50	31.5	1208.95	7.16	168.88
	SCR	14.95	500.681	8.00	62.58
July	N5	29.42	3479.69	21.21	164.04
	N9	83.16	3895.84	26.43	147.41
	S6	83.84	4399.22	30.73	143.17
	SCR(2)	9.99	792.06	4.823	164.24
Seawater	IAPSO*	35	1310	7.7	170.13

*IAPSO elemental concentrations are taken directly from GEOREM standards (Jochum et al., 2005).

Due to the above complications related to elemental concentration data for waters, using the data as a ratio such as Mg/Sr aids in the elimination of some of those issues that might impact data. Observing the data as a ratio rather than commenting on single element concentrations is able to occur as Sr and Mg seem to be affected similarly by the incorrect preparation methods and thus the integrity of the whole solution is preserved (see Figure 6 for outlier comparisons).

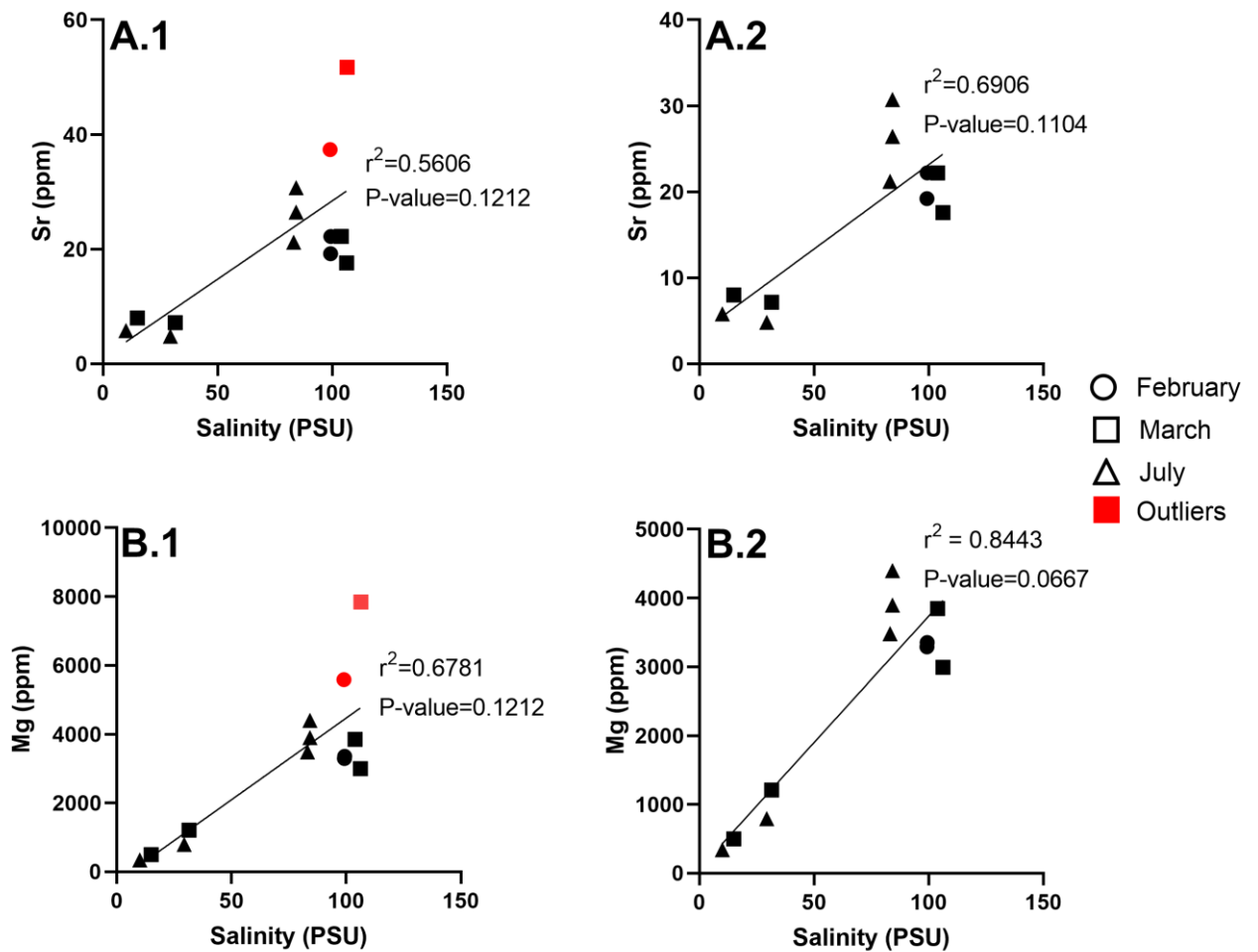


Figure 6. Elemental concentration of water samples against their salinity (in practical salinity units, PSU). A.1 and B.1 both show all water samples taken, data points in red were removed in A.2 and B.2 (same two data points in both A and B) showing a more linear relationship, suggesting the two data points omitted are outliers and thus making further inferences from elemental concentration data should be done so with caution.

Figure 6 shows a positive correlation between elemental concentration data and salinities and illustrates potential outlier data (red symbols – waters collected in February and March) in measured elemental concentrations. In future, additional acidification of February and March water samples (to redissolve any precipitates into solution) and follow up re-analysis by the ICP-MS could be done to perhaps improve confidence in the acquired data and to identify the primary cause for those outlier data.

4.1.2 MAGNESIUM AND STRONTIUM ELEMENTAL RATIOS IN SHELLS

Table 5 shows elemental concentration data for Sr and Mg, and calculated Mg/Sr ratios, with respect to shell weight. The Mg and Sr concentrations, and calculated Mg/Sr (ppm/ppm) ratios, within modern and fossil *A. helmsi* (Table 5) will be used in comparison with data from water samples (Table 3) to reconstruct possible temporal variations in Mg/Sr ratios. Specifically in palaeo-lagoon waters based on analysis of fossil shells collected from core-1, to infer and comment on potential human-induced palaeo-environmental changes. All elemental concentration data supplied comes from the same diluted solution.

Table 5. Elemental concentrations in parts per million (ppm) of modern and fossil shells sampled in March 2020 with corresponding core depth, back calculated from ICP-MS diluted concentrations with respect to shell weight.

	Core depth (cm)	Mg (ppm)	Sr (ppm)	Mg/Sr (ppm/ppm)
Modern	0	20.052	179.63	0.112
	0	36.49	333.26	0.110
	2	447.40	4317.51	0.104
	6	20.29	296.30	0.068
	10	50.87	627.04	0.081
	14	28.31	414.72	0.068
Fossil	18	28.20	478.24	0.059
	25	23.03	337.15	0.068
	30	293.07	4331.18	0.068
	40	31.85	436.47	0.073
	50	33.43	480.18	0.070
	55	42.11	490.83	0.086
	65	34.45	449.11	0.077
	70	18.85	244.82	0.077
	80	28.75	293.24	0.098
	80	16.92	187.24	0.090

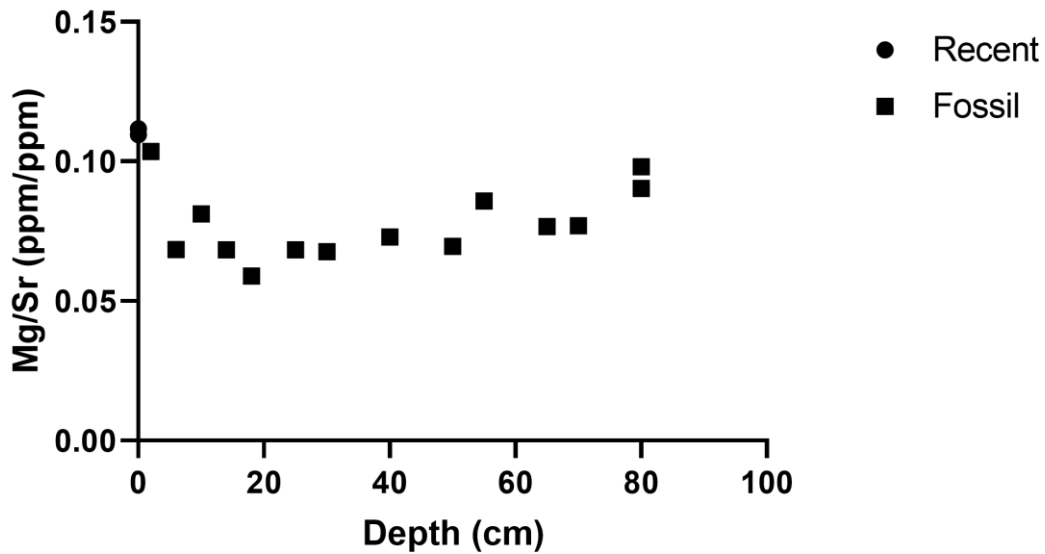


Figure 7. Elemental Mg/Sr (ppm/ppm) ratios of recent (circles) and fossil (square) shells plotted as a function of the core depth, where 80cm corresponds to an age of 3275 B.P. (Foster, et al. pers. comm. 2020) and modern shells were sampled in March 2020.

Figure 7 shows that Mg/Sr ratios of 0.110 ± 0.002 ppm/ppm in modern shells are systematically higher compared to the overall Mg/Sr ratio of 0.077 ± 0.013 ppm/ppm for fossil shells. Generally the Mg/Sr ratio in fossil shells shows an almost linear trend with time (i.e., depth), and thus appears relatively stable throughout core-1 with a slight positive shift to higher values in deeper sections of the core, i.e., from ~50cm onwards.

4.2 Radiogenic ($^{88}\text{Sr}/^{87}\text{Sr}$) and stable Strontium ($\delta^{88/86}\text{Sr}$) isotope data

The Sr isotopic signatures of recent water inputs into the Coorong Lagoon, hypothetical water source end-members (i.e., seawater, fresh/brackish water and hypersaline) are presented in Figure 8; derived from Shao et al. (2018); Shao et al. (Submitted). The Sr isotopic signatures of waters analysed in this study, as well as modern and fossil shells, are presented in sections below, with data listed in Tables 6 and 7, see also Figures 8 and 9. As to possible Sr isotope offsets between modern shells and water, these are

illustrated in Figure 10, and are used to quantify and reconstruct past changes in radiogenic and stable strontium isotope variations of palaeo-waters in Coorong Lagoon, with the same end-member water sources with shell isotopic variations also plotted in Figure 11.

4.2.1 STRONTIUM ISOTOPE VARIATIONS IN WATERS

Table 6 contains radiogenic and stable strontium isotopes data from recent waters, along with their salinity data (the latter also provided in Table 3), where the $^{87}\text{Sr}/^{86}\text{Sr}$ and $\delta^{88/86}\text{Sr}$ data from studied waters are also plotted with the above mentioned hypothetical end-member water sources in Figure 8.

Table 6. Recent water $\delta^{88/86}\text{Sr}$ (‰) and $^{88}\text{Sr}/^{87}\text{Sr}$ data measured by TIMS, and salinity data, with relative locations for samples available in Table 3, with relative water end-members from Shao et al. (Submitted).

Date	General Location	Sample Name	Salinity (PSU)	$\delta^{88/86}\text{Sr}$)%.(2*SE	$^{87}\text{Sr}/^{86}\text{Sr}$	2*SE
February 2020	South Lagoon	LZ 1	99	0.420	0.013	0.709252	0.000003
	South Lagoon	LZ 3	99.34	0.406	0.014	0.709254	0.000003
	South Lagoon	LZ 5	99.21	0.385	0.012	0.709234	0.000004
March 2020	South Lagoon	COOR - 01	103.88	0.370	0.014	0.709241	0.000004
	South Lagoon	COOR - 04	104.55	0.412	0.012	0.709249	0.000003
	South Lagoon	COOR - 07	104.89	0.347	0.012	0.709256	0.000003
	North Lagoon	COOR - 50	31.5	0.355	0.013	0.709196	0.000003
	Salt Creek Regulator	SCR	29.42	0.419	0.012	0.709260	0.000003
July 2020	North Lagoon	N5	83.16	0.395	0.013	0.709223	0.000187
	South Lagoon	N9	84.25	0.442	0.032	0.709261	0.000004
	South Lagoon	S6	83.84	0.426	0.032	0.709248	0.000003
	Salt Creek Regulator	SCR(2)	9.99	0.385	0.012	0.709271	0.000003
End-members	Hypersaline	-	-	0.415	-	0.709240	-
	Freshwater	-	-	0.300	-	0.709179	-
	Marine	-	-	0.385	-	0.709179	-

Note that a sample (S7 seen in July in Table 3) was removed from isotopic signatures because the double-spike was incorrectly applied and therefore the method for normalising the $\delta^{88/86}\text{Sr}$ was unable to be carried out (see Appendix C for further details on spike analysis).

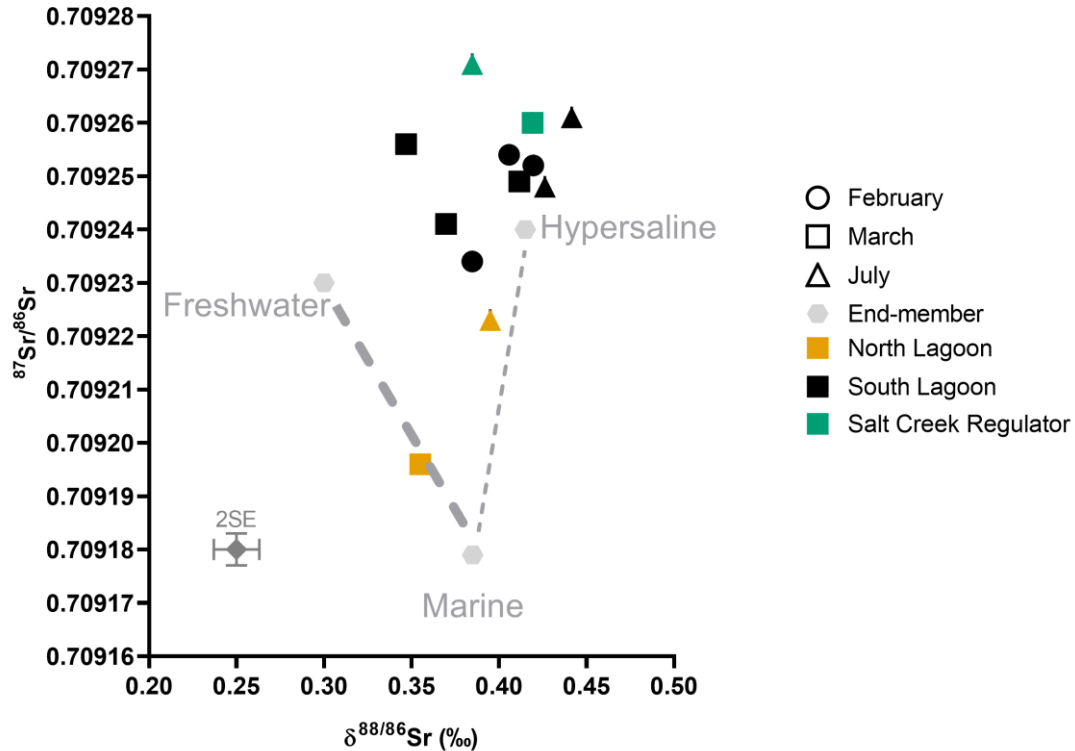


Figure 8. $^{87}\text{Sr}/^{86}\text{Sr}$ and $\delta^{88/86}\text{Sr}$ (‰) values for water samples taken in 2020 in Coorong Lagoon (this study), plotted together with hypothetical end-member water sources (marine, fresh and hypersaline waters), the latter adopted from stable and radiogenic Sr isotope data from Shao et al. (2018); (Shao et al., Submitted). Different shapes of symbols indicate different sampling campaigns (in February, March and July 2020), and different colour coding illustrates different sampling locations (i.e. North and South Lagoon and Salt Creek).

Coupled $^{87}\text{Sr}/^{86}\text{Sr}$ and $\delta^{88/86}\text{Sr}$ isotopic signature of the South Lagoon waters plot around the hypersaline end-member as illustrated in Figure 8. The North Lagoon samples plot further away from hypersaline end-member along the mixing line between hypersaline and marine, as well as between the two end-members of hypersaline and freshwater (see Table 6 for end-member values). The Salt Creek Regulator water that was sampled plotted with more radiogenic ($^{87}\text{Sr}/^{86}\text{Sr}$) values than any other studied water, but had similar $\delta^{88/86}\text{Sr}$ values to the bulk of the lagoon water data acquired from the Coorong, especially in the South Lagoon (see Figure 8).

4.2.2 STRONTIUM ISOTOPE VARIATIONS IN SHELLS

The Sr isotope results from modern shells collected from top sediment in March 2020 at site COOR – 50 in the North Lagoon, in March 2020, are listed in Table 7. The Sr isotope data from fossil shells which were sampled from the sediment core, core-1, in the South Lagoon are also listed below in Table 7. Note that sediment from core 1 at depth 80cm was dated via C¹⁴ method and this yielded an age of 3275 ± 25 years (before present, B.P.) (Foster, et al. pers. comm. 2020), and currently no other horizons are dated throughout this core.

Table 7. $\delta^{88/86}\text{Sr}$ (‰) and $^{88}\text{Sr}/^{87}\text{Sr}$ from modern and fossil shells from the Coorong Lagoons. Annotation of P or W in a sample name indicates whether the shells in this sample were classified as pink (P) or white (W), see also (Appendix A) for examples of colour separation.

Sample Type	Sample Name	Horizon depth (cm)	$\delta^{88/86}\text{Sr}$)‰(2*SE	$^{88}\text{Sr}/^{87}\text{Sr}$	2*SE
Modern	COOR-50-P	0	0.210	0.013	0.709233	0.000002
	COOR-50-W	0	0.257	0.016	0.709230	0.000003
Fossil	core 02	2	0.285	0.012	0.709243	0.000003
	core 06	6	0.225	0.014	0.709259	0.000239
	core 10	10	0.304	0.012	0.709253	0.000003
	core 14	14	0.290	0.016	0.709251	0.000230
	core 18	18	0.300	0.011	0.709255	0.000003
	core 25	25	0.284	0.020	0.709248	0.000199
	core 30	30	0.244	0.014	0.709259	0.000002
	core 40	40	0.248	0.017	0.709249	0.000180
	core 50	50	0.279	0.012	0.709255	0.000004
	core 55	55	0.282	0.013	0.709250	0.000232
	core 65	65	0.324	0.013	0.709240	0.000003
	core 70	70	0.326	0.013	0.709249	0.000189
	core-80-P	80	0.264	0.012	0.709252	0.000003
	core-80-W	80	0.298	0.016	0.709248	0.000003

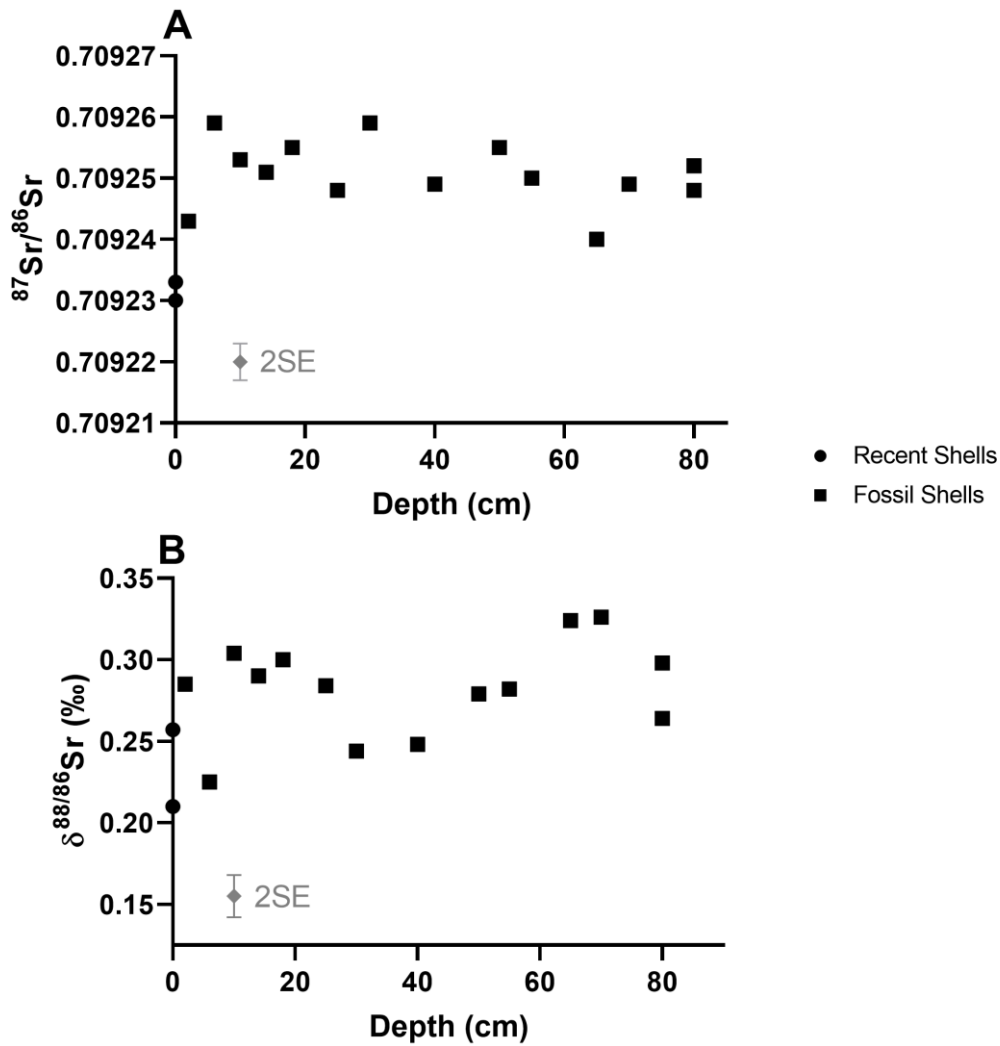


Figure 9. (A) $^{87}\text{Sr}/^{86}\text{Sr}$ and (B) $\delta^{88/86}\text{Sr}$ (‰) data from fossil shells with respect to core depth, where the depth of 80cm was dated at 3275 B.P. (Foster, et al., pers. comm. 2020), and modern shells were sampled in March 2020.

As to radiogenic Sr isotope variations, the $^{87}\text{Sr}/^{86}\text{Sr}$ signature in modern shells is ~0.709231 whereas on average the fossil shells have a slightly more radiogenic Sr isotope ratio of ~0.70925. For stable Sr isotopes, the $\delta^{88/86}\text{Sr}$ in modern shells is 0.233‰ whereas within the core the fossil shells data are on average around 0.282‰ (see Figure 10). The variation in both radiogenic and stable Sr data throughout core-1 is significant, especially when palaeo-hydrological inferences are being drawn from the data.

4.2.2.1 Sr isotope offsets between shells and water, and impact of colour variation

Offsets seen between modern shells and ambient waters are of particular interest because the same effect can be applied to infer Sr isotope composition of palaeo-lagoon waters based on the analysis of Sr isotopes in fossil shells. In this section radiogenic and stable Sr isotope data are plotted against latitude to observe differences between modern shells and recent lagoon water (see Figure 11). As indicated, the primary interest here is to compare and quantify Sr isotope data between modern shells and lagoon waters for the purposes of palaeo-water reconstruction.

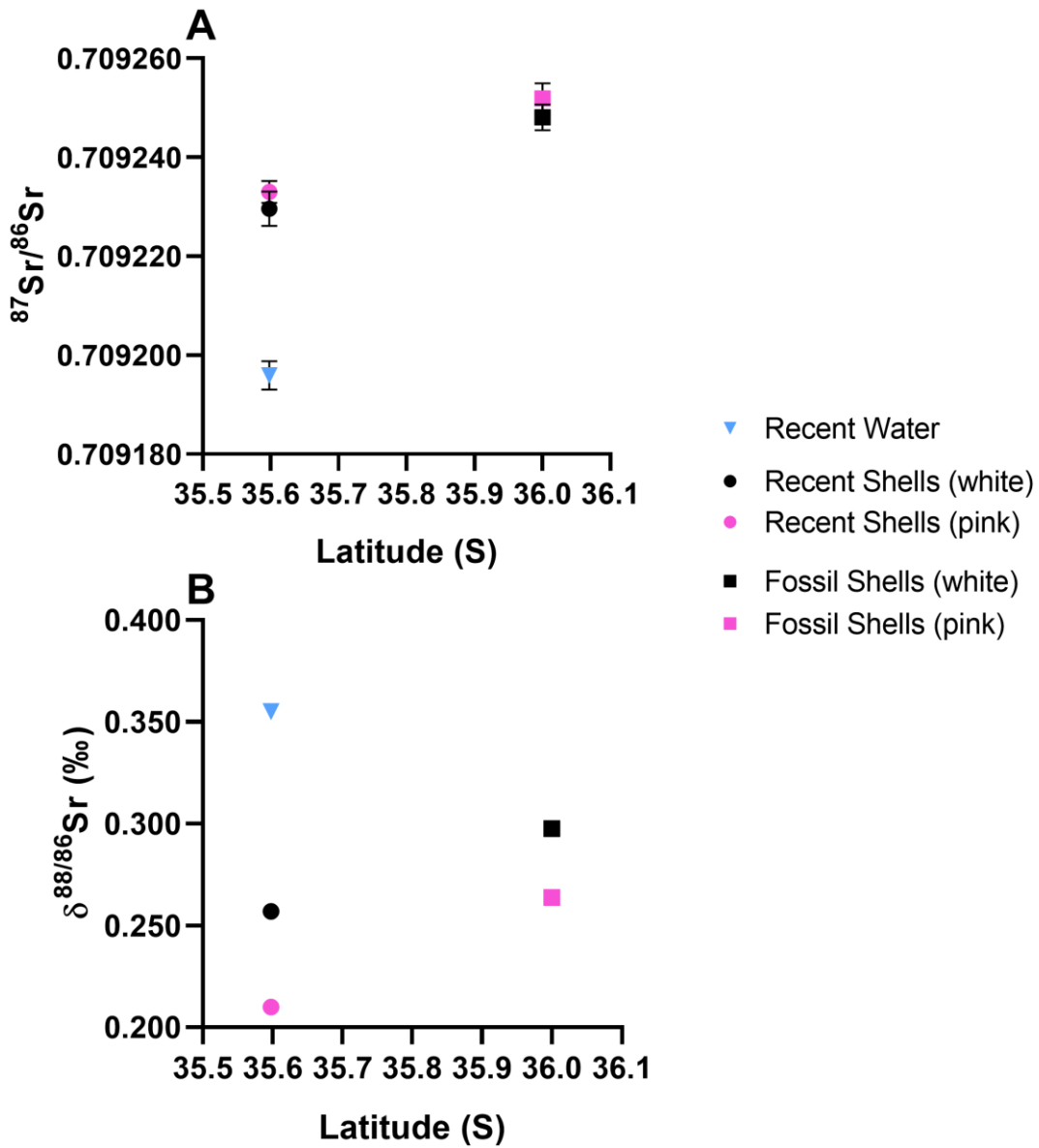


Figure 10. (A) $^{87}\text{Sr}/^{86}\text{Sr}$ and (B) $\delta^{88/86}\text{Sr}$ (‰) data from modern and fossil shells, along with recent water plotted spatially where modern shells have been sampled from the North Lagoon and fossil shells from the South Lagoon. Standard errors have been added to both A and B although the typical standard error is ± 0.013 for $\delta^{88/86}\text{Sr}$ (‰) data which is thus smaller than the symbols.

Table 8. Comparison of offset in $\delta^{88/86}\text{Sr}$ data between pink, white and a mixture of pink and white coloured shells; and the $\delta^{88/86}\text{Sr}$ (‰) of ambient lagoon waters to which shell data are compared to (i.e., to calculate the offsets), where the local waters has $\delta^{88/86}\text{Sr}$ (‰) signature of 0.355, see also data in Figure 10.

Modern shells	$\delta^{88/86}\text{Sr}$ (‰)	$\delta^{88/86}\text{Sr}$ (‰) Offset between shells and water
Pink	0.210	0.145
White	0.257	0.098
Average of pink and white	0.233	0.122

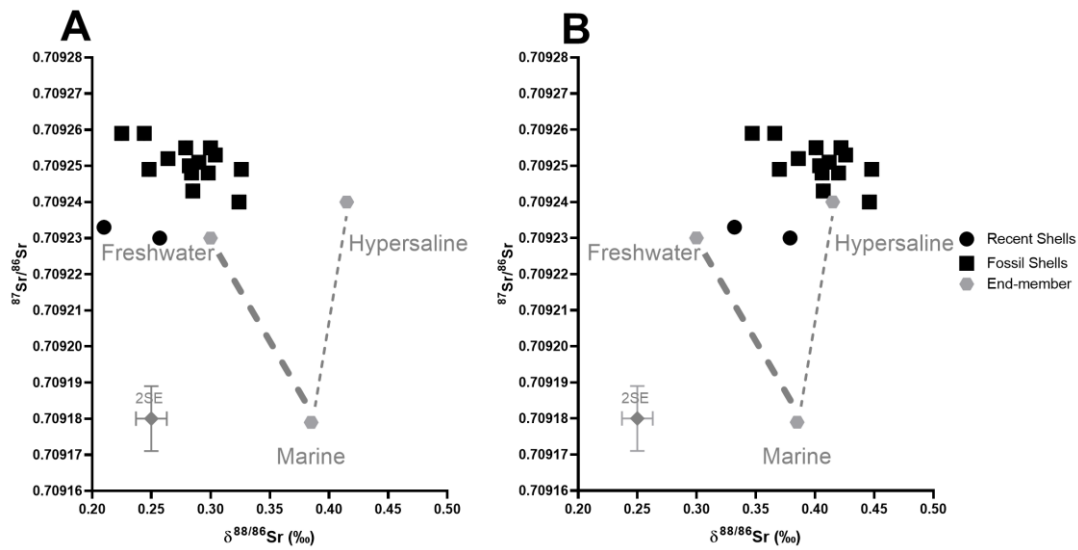


Figure 11. $^{87}\text{Sr}/^{86}\text{Sr}$ and $\delta^{88/86}\text{Sr}$ (‰) data of modern and fossil shells plotted in the three-isotope plot. Modern shells were collected from site COOR 50 in the North Lagoon and fossil shells were sampled from sediment core-1 in the South Lagoon. Freshwater, hypersaline and marine end-members are taken from Shao et al. (2018) and Shao et al. (Submitted). (A) Sr isotope data from shells with end-members with no offset applied to shell data, and in (B) an average offset of ± 0.122 ‰ was applied to fossil shell data to infer palaeo-water $\delta^{88/86}\text{Sr}$ signatures (see also data in Table 8).

Figure 11 displays the observed offsets in Sr isotope data between modern shell and recent water data for both radiogenic and stable Sr isotope results. The calculated average ‘offset values for stable Sr isotope data are listed in Table 8. An offset related to colouration variations of shells can also be seen in both fossil and modern shells but only in the stable strontium ($\delta^{88/86}\text{Sr}$) isotope data (Figure 10B), and not for radiogenic $^{87}\text{Sr}/^{86}\text{Sr}$ data where the difference is within the uncertainty of 0.000090 (Figure 10A and Table 2 for exact uncertainty). The specific offset that has been applied to Figure 13 is an average between the pink and white shells to make it more comparable to previous studies of the *A. helmsi*, for example Shao et al. (Submitted) shows a $\delta^{88/86}\text{Sr}$ offset between modern shells and local water of 0.1 to 0.2‰.

4.3 Coupled multi-proxy elemental (Mg/Sr) and Sr isotope approach

Using the above approach that is (i) outlining end-members of different water source input into the Coorong in the three-isotope Sr plot (i.e., $^{87}\text{Sr}/^{86}\text{Sr}$ vs. $\delta^{88/86}\text{Sr}$), coupled with (ii) an additional proxy data such as Mg/Sr ratios can help to further constrain palaeo-environmental and hydrological changes and plausible water source mixing scenarios based on the data. Note that unlike Sr concentrations in waters that are sensitive to changes due to precipitation of carbonates. Mg is a more conservative element as shown by its relationship to salinity in the Coorong Lagoon with a linear relationship and positive correlation (Figure 6). In addition, fresh/brackish waters from Salt Creek have very specific and anomalously low Mg/Sr ratios (compared to typical seawater or lagoon waters, Figure 12). Which thus helps to identify freshwater inputs in the Coorong Lagoon.

4.3.1 MULTI-PROXY APPROACH USING WATER DATA

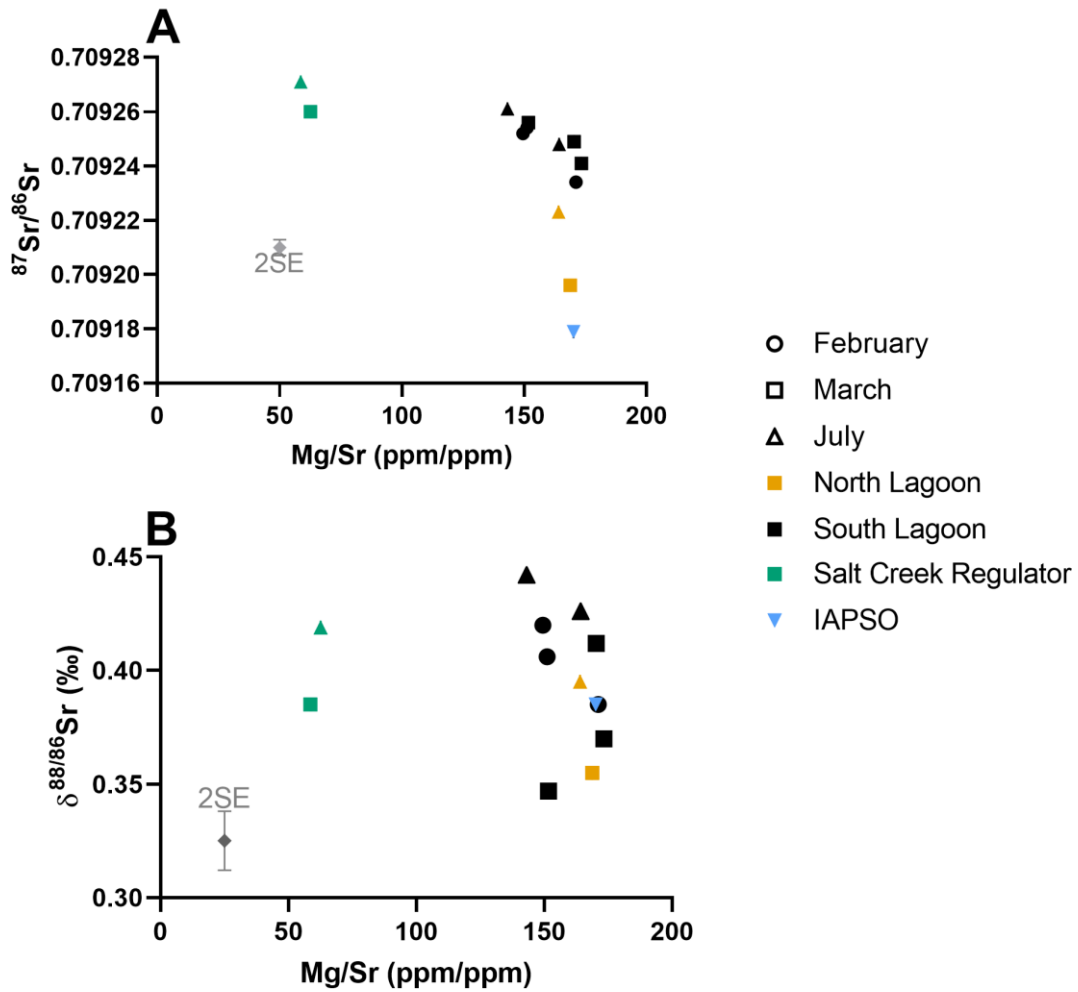


Figure 12. (A) $^{87}\text{Sr}/^{86}\text{Sr}$ ratios and (B) $\delta^{88/86}\text{Sr}$ (‰) data of recent waters from Coorong region, plotted against their Mg/Sr ratios.

The multi-proxy approach shown in Figure 12A, which combines Mg/Sr and Sr isotope data illustrates that in general waters from the North and South Lagoons can be explained by mixing of (i) fresh/brackish waters derived from the Salt Creek Regulator and (ii) seawater derived from Southern Ocean (blue triangle in Figure 12), which some additional effect such as carbonate precipitation that might also impact lagoon data.

4.3.2 MULTI-PROXY APPROACH USING SHELL DATA

The potential relationship and coupling between Mg/Sr and Sr isotope data, due to the above-mentioned water source mixing (i.e., seawater vs. freshwater) has been also expected for fossil shells data, as illustrated in Figures 13A and B.

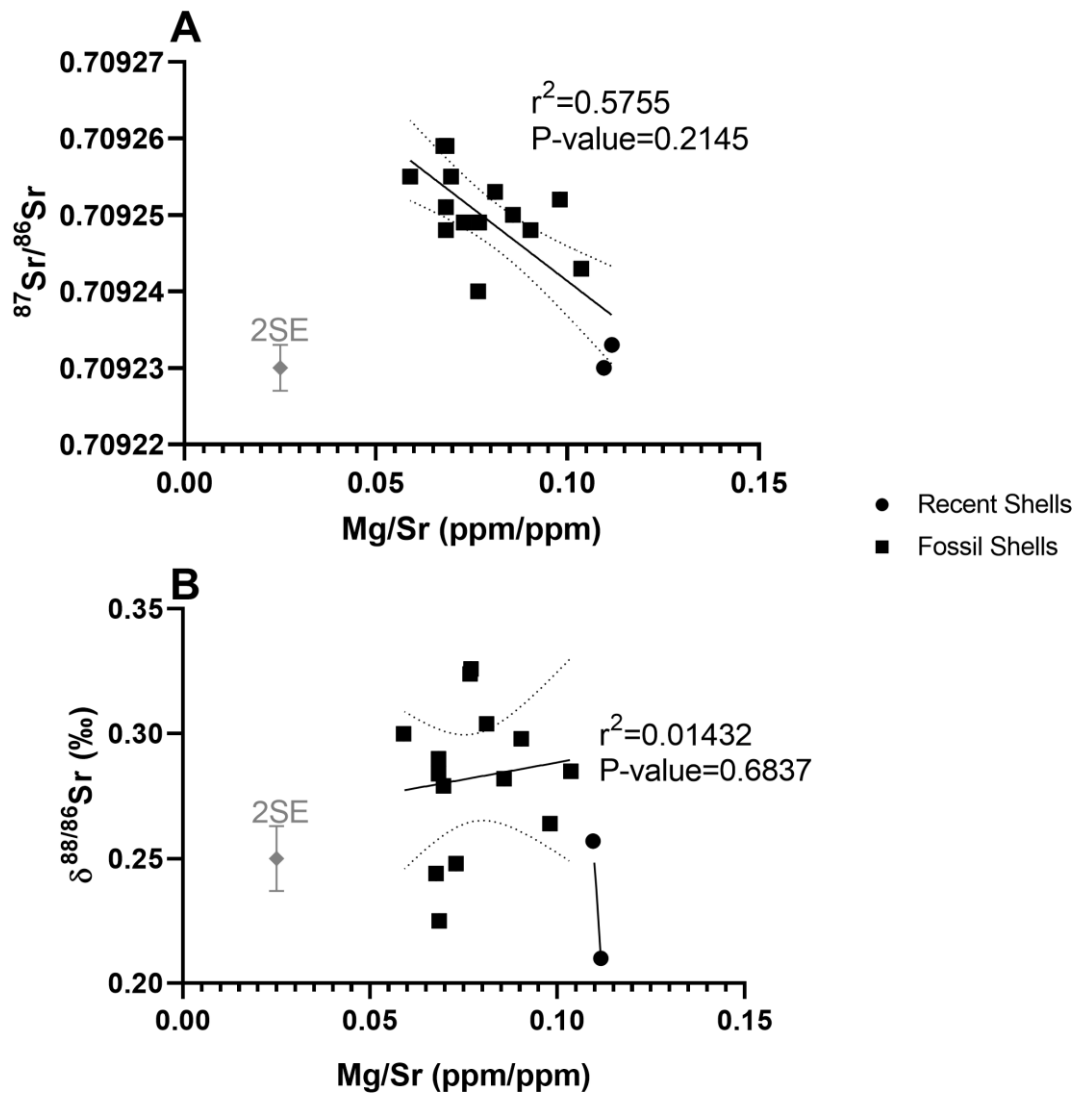


Figure 13. $^{87}\text{Sr}/^{86}\text{Sr}$ ratios and (A) and $\delta^{88/86}\text{Sr}$ (‰) data (B) of modern and fossil shells, plotted against their Mg/Sr elemental ratios.

Interestingly, an indication of a weak linear relationship and general anti-correlation has been observed for radiogenic $^{87}\text{Sr}/^{86}\text{Sr}$ and Mg/Sr data in shells of *A. helmsi* (see Figure

13A); however, stable Sr isotope data from shells are more scattered and show no clear relationship with Mg/Sr ratios (see Figure 13B).

5 DISCUSSION

The Coorong Lagoons represent a dynamic hydrological system that can be highly variable throughout annual seasons, years and even days (Mosley et al., 2018). This creates challenges in successfully representing the seasonal and spatial variations through such a small window of observation and data collection presented in this thesis. These natural variations are expected to be reflected in elemental concentrations and isotopic signatures of local lagoon waters due to the dynamic nature of this complex hydrological system. To address these challenges multiple sampling sites across the lagoon and various isotope tracers for water sources have been used in comparison to previous studies see Shao et al. (2018), Chamberlayne et al. (2019) and (Shao et al., Submitted), this study is building upon their pioneering work.

5.1 Radiogenic and stable Strontium isotope variations in Coorong waters and shells: Implications for local environmental conditions

Local water chemistry and salinity conditions are reflected in Sr isotopes in modern water and biogenic carbonates using a comparison between $^{87}\text{Sr}/^{86}\text{Sr}$ and $\delta^{88/86}\text{Sr}$ data of modern aragonitic shells of *A. helmsi* and ambient lagoon waters (collected in the North Lagoon, with ~32 PSU). Between these samples the radiogenic strontium isotope data ($^{87}\text{Sr}/^{86}\text{Sr}$) should display identical isotopic signatures. As any radiogenic Sr isotope anomalies in water should be directly reflected in $^{87}\text{Sr}/^{86}\text{Sr}$ data of shells, as generally any difference in the latter is observed in stable Sr ($\delta^{88/86}\text{Sr}$). The recent North Lagoon water sampled in 2020 yielded $^{87}\text{Sr}/^{86}\text{Sr}$ value of 0.709196, whilst the shell value was

0.709233, which is something that was not anticipated. Such difference in $^{87}\text{Sr}/^{86}\text{Sr}$ data between modern shells and ambient lagoon water (both sampled at the same time and location) has to be thus somehow controlled by changing water sources at this location throughout the year, considering that the shell of *A. helmsi* records a time period of about ~1 year, which is a typical life span of this bivalve species (Chamberlayne et al., 2019; Wells & Threlfall, 1982). During such prolonged period, the conditions and local isotope Sr signatures of waters can vary considerably due to changing inputs of freshwater from the Lower Lakes and seawater from the Southern Ocean, which both can vary seasonally. Such hypothetical mixing between different water sources is illustrated Figure 8 (see dashed lines), an indication of such mixing is also apparent from data of bivalve shells (Figure 11) that seem to plot between freshwater and seawater end-members; once the offset between shell to water has been applied. Stable strontium ($\delta^{88/86}\text{Sr}$) data in modern shells and ambient lagoon water show an offset that is quantifiable (Shao et al., Submitted; Vollstaedt et al., 2014). This offset can be explained by the effect of kinetic or biological isotope fractionation during the precipitation and bio-mineralization of carbonates/shells from ambient water or calcifying solution (Vollstaedt et al., 2014). Other parameters that could also affect such stable Sr isotope fractionation during carbonate formation include pH, temperature, and salinity. In the Coorong Lagoon it is difficult to constrain all variables that contribute towards understanding how stable Sr isotopes might respond and fractionate in this complex and dynamic hydrological system (Mosley et al., 2018; Shao et al., 2018; Singurindy et al., 2004).

5.2 Impact of high versus low flow of freshwater via Salt Creek on strontium isotope composition into the South Lagoon

High seasonal variability of the Coorong's South Lagoon flow rate from the Salt Creek Regulator Flow is presented in Figure 14. Overall, the flow rate passing through the Salt Creek Regulator during the 2020 sampling period provided less freshwater to the South Lagoon in comparison to the previous year. Freshwater flow coming into the South Lagoon from Salt Creek in 2020 did increase during the winter months, but only marginally (see data in Figure 14). During summer, or low flow stable strontium is more concentrated due to reduction in water flow and increase in evaporation and thus the lighter ^{86}Sr isotope preferentially precipitate into carbonates such as *A. helmsi*. Throughout winter, flow rates generally increase in comparison to summer, however comparing the two winter periods observed in Figure 14 the fluctuation between two winters is also variable.

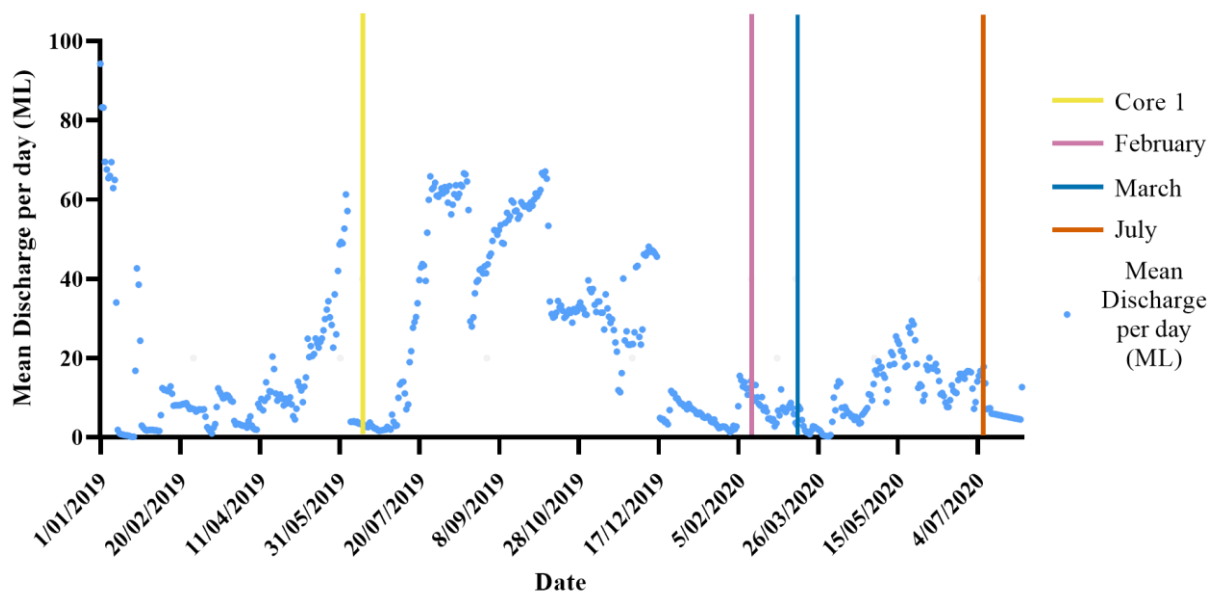


Figure 14. Water flow rate in mega litres (ML) per day at the government controlled Salt Creek Regulator (SCR) during the period of time that samples of waters for this study were taken in 2020 February, March and July; along with levels when core-1 was taken in 2019 (yellow line). It is worth mentioning that the average flow rate during 2019 May and June (when core-1 was taken)

has been around 17 ML of water per day through the SCR and the months (Department of Environment and Water, 2020).

The sampling regime displayed in this thesis saw only a small variation in freshwater input from the South Lagoon. Thus potentially explaining the little difference seen in regards to radiogenic signatures (Figure 8) in comparison to seasonal change during 2020 because of only a marginal change in continental freshwaters. The differences between flow rates are much greater in 2019 than in 2020 (see Figure 14).

5.3 Variability in radiogenic and stable Sr isotope data in lagoon waters, as well as modern and fossil carbonate shells, from the Coorong Lagoons.

As mentioned above seasonal fluctuations directly affects the variability of radiogenic and stable Sr isotopes within the South Lagoon mostly due to freshwater input from Salt Creek in combination with a relatively unknown amount of freshwater coming from the groundwater aquifer below (Shao et al. submitted). Radiogenic Sr variation differentiates end-members with marine radiogenic signature of 0.709179 compared to hypersaline and freshwater with 0.709240 and 0.709230 respectively. When observing temporally different shells the variation in $^{87}\text{Sr}/^{86}\text{Sr}$ is due to percentage of water mixed from seawater with 0.709179 radiogenic Sr and Salt Creek with ~ 0.709266 radiogenic Sr. This is one of the reasons why the difference between freshwater and hypersaline is nominal if you were to solely observe this ratio without the aid of stable Sr ($\delta^{88/86}\text{Sr}$). Stable Sr acts as a proxy for salinity as this affects carbonates preferential precipitation of lighter $\delta^{88/86}\text{Sr}$ from the water source they inhabit (Shao et al. submitted).

5.4 Quantifying the $\delta^{88/86}\text{Sr}$ isotope fractionation between water and shells

The offset between $\delta^{88/86}\text{Sr}$ data of present-day lagoon water and modern shells of *A. helmsi* is important to constrain and quantify, as knowledge of this offset is important for reconstructions of stable Sr isotope composition of palaeo-waters based on analysis of fossil shells (see also Shao et al. (Submitted)). Following this approach, and assuming that such offset remained constant over time, one can use $\delta^{88/86}\text{Sr}$ data of fossil shells to model palaeo-water Sr isotope signatures based on analysis of shells of *A. helmsi* (see Figure 11A without the offset; and Figure 11B with the offset applied). In this study, we found that the offset or difference between stable Sr isotope values of modern shells and lagoon water is $\sim 0.122\text{‰}$ (water being isotopically heavier than the shells). This is consistent with data from Shao et al. (Submitted) that reports a difference in stable Sr isotope composition between lagoon waters and modern *A. helmsi* shells between 0.1 and 0.15‰. These offsets are however slightly lower than those found in marine environments recorded by Fruchter et al. (2016), which are on the order of $\sim 0.2\text{‰}$, suggesting possible species-specific control on stable Sr isotopes in biogenic carbonates.

5.5 Assessing the effect of European settlement on the Sr isotope record of shells and palaeo-waters in the Coorong

This thesis aimed to have more ^{14}C dates available from core-1, to better constrain where specifically the core records the onset of European settlement (pre 1800's) in South Australia, in relation to specific depth (cm) of the sediment core. Whilst the single available ^{14}C date of ~ 3275 years B.P. (at the base of the core) provides an important time horizon or reference point for generated Sr isotope and Mg/Sr data, this single age

is obviously not sufficient to constrain the horizons recording the European settlement, the latter documented around 1800. Thus the exact horizon depth ~220 years ago, when the Coorong Lagoon system start experiencing the impact of anthropogenic change is currently unknown and needs to be constrained in future with more ^{14}C dating.

Nevertheless, a comparison of relative changes in Sr isotope and Mg/Sr data of fossil shells over time, as well as comparison of modern versus fossil shells data, is still relevant and important as it can provide information on relative changes in palaeo-environmental and hydrological conditions; even without the knowledge of absolute ages. These temporal trends or time-series of $^{87}\text{Sr}/^{86}\text{Sr}$ and $\delta^{88/86}\text{Sr}$ and Mg/Sr data, acquired from fossil shells, are present in Figure 9 and Figure 11A and B. Whilst there are obvious differences between data acquired from modern and fossil, there are also detectable and possibly systematic variations in Sr isotope data and Mg/Sr ratios in time-series data from fossil shells, implying plausible temporal changes in water sources and their relative mixing in the Coorong South Lagoon.

5.6 Modelling water mixing and palaeo-salinity in Coorong South Lagoon

Apportioning water source and their relative mixing, and inferring palaeo-salinity in the lagoon, requires some assumptions for mass balance calculations to reconstruct changes in water mixing and salinity in the South Lagoon characteristics. Such modelling approaches can be based on multi-proxy data, including Sr isotope and Mg/Sr records, based on analysis of fossil and modern shells, and inferred $^{87}\text{Sr}/^{86}\text{Sr}$, $\delta^{88/86}\text{Sr}$ and Mg/Sr signatures of palaeo-lagoon waters (see Figures 13 and 14).

5.6.2 ELEMENTAL AND ISOTOPE MASS BALANCE OF STRONTIUM IN THE COORONG LAGOON

A mass balance equation, for a simple two-component mixing between seawater (SW) and freshwater (Salt Creek –SC) is shown below (see Equation 3).

Equation 3

$$Sr_{(mix)} = (F_{SC} * Sr_{SC}) + (F_{SW} * Sr_{SW})$$

Where Sr(mix) is the concentration of Sr in ppm in the mixture or lagoon water, and Sr(SC) and SR(SW) respectively represent the Sr concentration in Salt Creek and Seawater, these abbreviations follow for Equation 4 as well. Isotope mass balance of Sr in the Coorong Lagoon is found using Equation 4 (modified from Farkaš et al. (2007); Shao et al. (2018), illustrated below, which can be used for both radiogenic ($^{87}\text{Sr}/^{86}\text{Sr}$) and ($\delta^{88/86}\text{Sr}$) isotope tracers. Equation 4 below is for radiogenic Sr isotopes, but can be adopted for stable Sr isotopes by simply replacing parameters labelled as $^{87}\text{Sr}/^{86}\text{Sr}$ (written as $^{87/86}\text{Sr}$) for $\delta^{88/86}\text{Sr}$.

Equation 4

$$^{87/86}Sr_{(mix)} = \frac{(F_{SC} * ^{87/86}Sr_{SC} * Sr_{SC}) + (F_{SW} * ^{87/86}Sr_{SW} * Sr_{SW})}{(F_{SC} * Sr_{SC}) + (F_{SW} * Sr_{SW})}$$

The above Equations 3 and 4, were used to generate and calculate theoretical mixing line for Sr concentrations and isotopes, as a result of a simple two-component mixing between seawater (SW) and freshwater (Salt Creek) end-members (see blue lines in Figure 15). Note that similarly to stable Sr isotopes (which show offset between $\delta^{88/86}\text{Sr}$ of shells and waters), the Mg/Sr elemental ratios also show offset between shells and ambient waters. A species specific ‘partitioning coefficient’ or factor seen in Equation 5 is applied to fossil shells Mg/Sr data to reconstruct the Mg/Sr ratio in palaeo-waters (see data in Figure 15).

Equation 5

$$\frac{Mg/Sr_{(shell)}}{Mg/Sr_{(water)}} = 0.001229$$

Where $Mg/Sr_{(shell)}$ is the ratio of Magnesium to Strontium in shells and the same element ratio is used for shells in $Mg/Sr_{(water)}$.

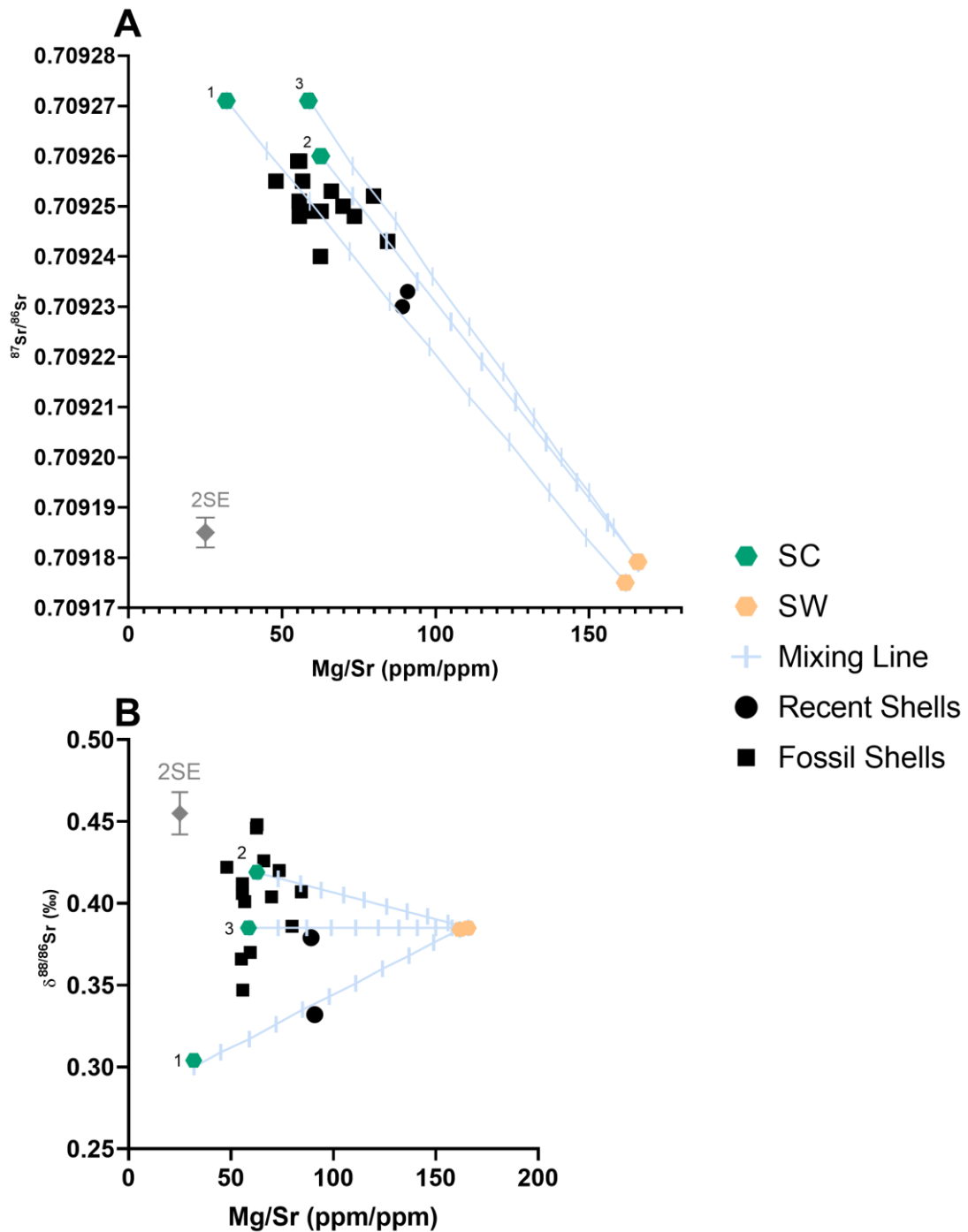


Figure 15. Cross-plots of $^{87}\text{Sr}/^{86}\text{Sr}$ (A) and $\delta^{88/86}\text{Sr}$ (B) versus Mg/Sr data in waters, based on fossil shells data with average offset of 0.122‰ for $\delta^{88/86}\text{Sr}$ applied to shells, and a partitioning coefficient for Mg/Sr ratio of 0.00123 (ppm/ppm). The blue lines represent various ‘mixing lines’ or scenarios between freshwater of Salt Creek (SC) and seawater (SW) end-members, where the tick marks illustrate 10% increments of SW and/or SC fractions (defined by F in Equation 4 above) in the theoretical mixtures. Along these mixing lines if palaeo-water (inferred from fossil shell data) were to plot on the SC member then that would indicate the shell existed in an environment that is made up from 100% Salt Creek derived Sr, and 0% seawater derived Sr, with the assumption the offset

and partitioning coefficient (shell vs. water) remained constant over time. Numerical annotation next to each mixing line represent scenarios for the following SC end-members: (1) Winter data provided by Shao et al. submitted, (2) Summer data (n=1) from this study and (3) Winter data (n=1) from this study.

Regardless of the mixing scenario selected (see below, Mixing Lines 1,2 and 3 for SC) the results of our mass balance calculations and fossil-based reconstruction of Coorong palaeo-waters (see black squares in Figure 15), our results indicate that the Coorong South Lagoon was never marine or dominated by typical seawater, at least over the last ~3275 years. Interestingly, our modelling also seems to indicate that Sr in the south Lagoon palaeo-waters was mostly dominated by the continental or Salt Creek derived Sr (ranging between ~75% up to ~90%), with only relatively minor contribution (between ~10% to ~25%) from the seawater-derived Sr sources (see data in Figure 15).

5.6.2 STRONTIUM ISOTOPE CONSTRAINTS ON THE PALAEO-SALINITY IN THE COORONG SOUTH LAGOON

Modelling the relative fractions (F) of Sr in the Coorong palaeo-waters, derived from seawater (SW) versus freshwater from Salt Creek (SC) inputs, an estimated plausible palaeo-salinity in the Coorong Lagoon can be found through using water mass balance calculations such as Equation 5. Knowing the fractions (F) as well as Sr concentrations in SW and SC end-members, can be translated to expected fractions or volumes of waters (SC vs SW) that were mixed to produce the observed Sr isotope and Mg/Sr mixing data (Figure 15). Based on $^{87}\text{Sr}/^{86}\text{Sr}$ and Mg/Sr palaeo-water from Figure 15A (black squares and mixing lines 1 and 3) a maximum contribution of SC derived Sr can be inferred, and thus a proportion of SC water can be inferred. Thus finding ~75% to 90% of water coming from SC and ~10-25% derived from SW. This would correspond to minimum palaeo-salinities in the Coorong South Lagoon on the order of only ~10 to

15 PSU (see calculated values in Table 9). These modelled findings assume that the concentrations of Sr in SC and SW were approximately equal. This is not unreasonable (see data in Table 4, and 9). Finding this assumption reasonable allows a direct relation of Sr fractions (F) to water fractions, and thus salinity, using the equation below:

Equation 6

$$\text{Paleo} - \text{salinity (mix)} = (F_{SW} * \text{Salinity}_{SW}) + (F_{SC} * \text{Salinity}_{SC})$$

Where palaeo-salinity (mix) is the calculated lagoon water mixture salinity (in PSU) and F is the fraction of seawater (SW) and freshwater (from Salt Creek - SC), with their respective salinities (in PSU).

Table 9. Palaeo salinity according to mixing line 1, 2 and 3. Fraction of seawater (SW) and fraction of Salt Creek (SC) waters plotted in in Figure 15 according to radiogenic, stable strontium and Mg/Sr ratios in recorded data used to infer palaeo salinity in partial salinity in practical salinity units (PSU) calculated via Equation 5.

Fraction of SW (%)	Fraction of SC (%)	⁸⁷Sr/⁸⁶Sr mix	Sr conc. mix	Calculated palaeo-salinity (PSU)
Mixing Line 1				
0	100	0.709271	7.70	7.18
10	90	0.709261	7.74	9.96
20	80	0.709251	7.78	12.74
30	70	0.709241	7.82	15.53
40	60	0.709231	7.86	18.31
Mixing Line 2				
0	100	0.709210	6.90	12.47
10	90	0.709206	7.04	14.72
20	80	0.709202	7.18	16.98
30	70	0.709199	7.33	19.23
40	60	0.709196	7.47	21.48
Mixing Line 3				
0	100	0.709260	8.00	14.95
10	90	0.709252	8.03	16.96
20	80	0.709243	8.07	18.96
30	70	0.709235	8.10	20.97
40	60	0.709227	8.13	22.97

Calculations in Table 9 outline the minimal plausible salinity scenarios for mixing lines 1, 2 and 3 respectively in the past Coorong South Lagoon, based on our palaeo-water data reconstructed from Sr isotope and Mg/Sr ratios of fossil shells. This does not account for other environmental effects on salinity concentration such as the relationship between evaporation and flow rate.

6 CONCLUSIONS

This study used radiogenic and stable strontium isotopes ($^{87}\text{Sr}/^{86}\text{Sr}$ and $\delta^{88/86}\text{Sr}$), complemented by Mg/Sr ratios, as an index for water mixing and freshwater vs marine input tracer into the present-day Coorong Lagoon. Applying this calibration of water sources, modern shells and salinity in the Coorong Lagoons to fossil carbonate shells of bivalve *Arthritica Helmsi* was then used for palaeo-salinity reconstructions by observing $^{87}\text{Sr}/^{86}\text{Sr}$, $\delta^{88/86}\text{Sr}$ and Mg/Sr. Using the latter multi-proxy approach was applied with a simple mass balance model to reconstruct palaeo-hydrological conditions (i.e., past changes in water source mixing). From this a palaeo-salinity can be inferred throughout the last ~3275 years and thus including a pre- and post-European settlement plausible minimum salinity of the South Lagoon. Importantly, results of this study confirmed that over the above period the waters in the Coorong South Lagoon were never ‘typically’ marine or dominated by seawater inputs, but rather complex mixtures of continental freshwaters with variable but relatively minor seawater inputs (i.e., ~10 to 20% fraction of seawater-derived Sr). The main water source into the past Coorong South Lagoon seems to be mostly fresh/brackish water supplied by Salt Creek (with >80% fractions), based on the Sr isotope and Mg/Sr ratio constrains. These tracers

coupled with mass balance calculations allowed for minimum estimates of plausible paleo-salinity levels in the Coorong South Lagoon, which could have been as low as 10 to 15 PSU, assuming no effects of water evaporation and/or carbonate formation on the Sr isotope and elemental ratio data.

This model and palaeo-salinity estimates should however be used with caution and the above assumptions as well as unconstrained inputs from local groundwater and/or rainfall should also be investigated. The South Lagoon is currently classified as permanently hypersaline, which based on our data and reconstructions was not a natural state of this unique Coorong Lagoon system prior to European settlement. Restoring the above and purported brackish salinity (~10-15 PSU) in the South Lagoon would require significantly higher freshwater flows from the Salt Creek. Future work and constraints on the local groundwater and rainfall inputs of freshwater into the Coorong can be used, in conjunction with data presented in this study, to further improve our understanding of this unique and dynamic hydrological system, which would be critical to improve its future management strategies and sustainability as a healthy ecosystem.

7 ACKNOWLEDGMENTS

I would like to acknowledge the diligent supervision of Juraj Farkaš, Jonathon Tyler, Luke Mosley and Bronwyn Gillanders as my main supervisors for this project along with Yuexiao (Mandy) Shao and Nicole Foster for providing me with invaluable help. I would like to thank; David Bruce for TIMS training, clean lab coordination and fielding my questions; Stacey Priestley for proper sampling and collection techniques of field samples, Gary Hera-Singh and Glen Hill for their unrivalled navigation of the Coorong Lagoon waters which aided sample collection efficiency, Sarah Gilbert at Adelaide Microscopy for training on and use of ICP-MS and her expertise in the preparation of solutions and Tony Hall for general lab training.

I would like to acknowledge the land and country sampled as that of the First Nations of the South East and the Ngarrindjeri people.

This research project, including the sampling and analysis of waters, has been supported by the Government of South Australia, Department of Environment and Water under their Project Coorong and its Healthy Coorong Healthy Basin (HCHB) initiative (<https://www.environment.sa.gov.au/topics/coorong>; <https://www.environment.sa.gov.au/topics/coorong/healthy-coorong-healthy-basin>); and analytical work on modern and fossil shells has been partly supported via Czech Science Foundation (GACR grant) and internal funding of University of Adelaide.

8 REFERENCES

- ANDREWS, M. G., JACOBSON, A. D., LEHN, G. O., HORTON, T. W., & CRAW, D. (2016). Radiogenic and Stable Sr Isotope Ratios ($^{87}\text{Sr}/^{86}\text{Sr}$, $\Delta^{88}\text{Sr}/^{86}\text{Sr}$) as Tracers of Riverine Cation Sources and Biogeochemical Cycling in the Milford Sound Region of Fiordland, New Zealand. *Geochimica et Cosmochimica Acta*, 173, 284-303. doi:10.1016/j.gca.2015.10.005
- BOURMAN, R. P., & BARNETT, E. J. (1995). Impacts of River Regulation on the Terminal Lakes and Mouth of the River Murray, South Australia. *Australian Geographical Studies*, 33(1), 101-115. doi:10.1111/j.1467-8470.1995.tb00688.x
- BROOKES, J. D., LAMONTAGNE, S., ALDRIDGE, K. T., BENDER, S., BISSETT, A., BUCATER, L., CHESHIRE, A. C., COOK, P. L. M., DEEGAN, B. M., DITTMANN, S., FAIRWEATHER, P. G., FERNANDES, M. B., FORD, P. W., GEDDES, M. C., GILLANDERS, G. M., GRIGG, N. J., HAESE, R. R., KRULL, E., LANGLEY, R. A., LESTER, R. E., LOO, M., MUNRO, A. R., NOELL, C. J., NAYAR, S., PATON, D. C., REVILL, A. T., ROGERS, D. J., ROLSTON, A., SHARMA, S. K., SHORT, D. A., TANNER, J. E., WEBSTER, I. T., WELLMAN, N. R., & YE, Q. (2009). An Ecosystem Assessment Framework to Guide Management of the Coorong. Final Report of the Cllammecology Research Cluster. . *CSIRO*. doi:10.4225/08/585ac4318b01f
- CAPO, R. C., STEWART, B. W., & CHADWICK, O. A. (1998). Strontium Isotopes as Tracers of Ecosystem Processes: Theory and Methods. *Geoderma*, 82, 197-225.
- CHAMBERLAYNE, B. K., TYLER, J. J., & GILLANDERS, B. M. (2019). Environmental Controls on the Geochemistry of a Short-Lived Bivalve in Southeastern Australian Estuaries. *Estuaries and Coasts*, 43(1), 86-101. doi:10.1007/s12237-019-00662-7
- DEPARTMENT OF ENVIRONMENT AND WATER. (2020). Water Connect Salt Creek Regulator. Access Date: 17 August. Retrieved from [https://www.waterconnect.sa.gov.au/Systems/SiteInfo/Pages/Default.aspx?site=A2390568&period=HRLY#Real-Time%20Data%20Plot,Real-Time%20Data%20Plot,Real-Time%20Data,Historic%20Data,Site%20Summary,Historic%20Data,Parameter%20Summary,Real-Time%20Data,Real-Time%20Data%20Plot,Historic%20Site%20Status,Site%20Summary,Real-Time%20Data,Historic%20Data%3E%20\[Accessed%2029%20April%202020,Site%20Photos,Parameter%20Summary,Historic%20Data,Real-](https://www.waterconnect.sa.gov.au/Systems/SiteInfo/Pages/Default.aspx?site=A2390568&period=HRLY#Real-Time%20Data%20Plot,Real-Time%20Data%20Plot,Real-Time%20Data,Historic%20Data,Site%20Summary,Historic%20Data,Parameter%20Summary,Real-Time%20Data,Real-Time%20Data%20Plot,Historic%20Site%20Status,Site%20Summary,Real-Time%20Data,Historic%20Data%3E%20[Accessed%2029%20April%202020,Site%20Photos,Parameter%20Summary,Historic%20Data,Real-)

[Time%20Data,Real-Time%20Data%20Plot,Historic%20Site%20Status,Historic%20Data](#)

- FARKAŠ, J., BÖHM, F., WALLMANN, K., BLENKINSOP, J., EISENHAUER, A., VAN GELDERN, R., MUNNECKE, A., VOIGT, S., & VEIZER, J. (2007). Calcium Isotope Record of Phanerozoic Oceans: Implications for Chemical Evolution of Seawater and Its Causative Mechanisms. *Geochimica et Cosmochimica Acta*, 71(21), 5117-5134. doi:10.1016/j.gca.2007.09.004
- FIETZKE, J., & EISENHAUER, A. (2006). Determination of Temperature-Dependent Stable Strontium Isotope ($^{88}\text{Sr}/^{86}\text{Sr}$) Fractionation Via Bracketing Standard Mc-Icp-Ms. *Geochemistry, Geophysics, Geosystems*, 7(8), n/a-n/a. doi:10.1029/2006gc001243
- FRUCHTER, N., EISENHAUER, A., DIETZEL, M., FIETZKE, J., BÖHM, F., MONTAGNA, P., STEIN, M., LAZAR, B., RODOLFO-METALPA, R., & EREZ, J. (2016). $^{88}\text{Sr}/^{86}\text{Sr}$ Fractionation in Inorganic Aragonite and in Corals. *Geochimica et Cosmochimica Acta*, 178, 268-280. doi:10.1016/j.gca.2016.01.039
- FUKAI, R., YOKOYAMA, T., & KAGAMI, S. (2017). Evaluation of the Long-Term Fluctuation in Isotope Ratios Measured by Tims with the Static, Dynamic, and Multistatic Methods: A Case Study for Nd Isotope Measurements. *International Journal of Mass Spectrometry*, 414, 1-7. doi:10.1016/j.ijms.2016.12.016
- GILLANDERS, B. M., & MUNRO, A. R. (2012). Hypersaline Waters Pose New Challenges for Reconstructing Environmental Histories of Fish Based on Otolith Chemistry. *Association for the Sciences of Limnology and Oceanography, Inc.*, 57(4), 1136-1148. doi:10.4319/lo.2012.57.4.1136
- HAYNES, D., SKINNER, R., TIBBY, J., CANN, J., & FLUIN, J. (2011). Diatom and Foraminifera Relationships to Water Quality in the Coorong, South Australia, and the Development of a Diatom-Based Salinity Transfer Function. *Journal of Paleolimnology*, 46(4), 543-560. doi:10.1007/s10933-011-9508-y
- HODELL, D. A., MEAD, G. A., & MUELLER, P. A. (1990). Variation in the Strontium Isotopic Composition of Seawater (8 Ma to Present) : Implications for Chemical Weathering Rates and Dissolved Fluxes to the Oceans. *Chemical Geology*, 80, 291-307. doi:10.1016/0168-9622(90)90011-Z
- JAMES, N. P., & BONE, Y. (2011). *Neritic Carbonate Sediments in a Temperate Realm*. In SPRINGER (Ed.), (pp. 264). doi:10.1007/978-90-481-9289-2
- JOCHUM, K. P., NOHL, U., HERWIG, K., LAMMEL, E., STOLL, B., & HOFMANN, A. (2005). Georem: A New Geochemical Database for Reference Materials and Isotopic Standards. *Geostandards and Geoanalytical Research*, 29(3), 333-338. doi:10.1111/j.1751-908X.2005.tb00904.x
- KINGSFORD, R. T., WALKER, K. F., LESTER, R. E., YOUNG, W. J., FAIRWEATHER, P. G., SAMMUT, J., & GEDDES, M. C. (2011). A Ramsar Wetland in Crisis - the Coorong, Lower Lakes and Murray Mouth, Australia. *Marine and Freshwater Research*, 62(3), 255-265. doi:10.1071/MF09315
- KOBER, B., SCHWALB, A., SCHETTLER, G., & WESSELS, M. (2007). Constraints on Paleowater Dissolved Loads and on Catchment Weathering over the Past 16 ka from $^{87}\text{Sr}/^{86}\text{Sr}$ Ratios and Ca/Mg/Sr Chemistry of Freshwater

- Ostracode Tests in Sediments of Lake Constance, Central Europe. *Chemical Geology*, 240(3-4), 361-376. doi:10.1016/j.chemgeo.2007.03.005
- KRABbenhöft, A., Eisenhauer, A., Böhm, F., Vollstaedt, H., Fietzke, J., Liebetrau, V., Augustin, N., Peucker-Ehrenbrink, B., Müller, M. N., Horn, C., Hansen, B. T., Nolte, N., & Wallmann, K. (2010). Constraining the Marine Strontium Budget with Natural Strontium Isotope Fractionations ($^{87}\text{Sr}/^{86}\text{Sr}^*$, $\Delta^{88}/^{86}\text{Sr}$) of Carbonates, Hydrothermal Solutions and River Waters. *Geochimica et Cosmochimica Acta*, 74(14), 4097-4109. doi:10.1016/j.gca.2010.04.009
- KRABbenhöft, A., Fietzke, J., Eisenhauer, A., Liebetrau, V., Böhm, F., & Vollstaedt, H. (2009). Determination of Radiogenic and Stable Strontium Isotope Ratios ($^{87}\text{Sr}/^{86}\text{Sr}$; $\Delta^{88}/^{86}\text{Sr}$) by Thermal Ionization Mass Spectrometry Applying an $^{87}\text{Sr}/^{84}\text{Sr}$ Double Spike. *Journal of Analytical Atomic Spectrometry*, 24(9). doi:10.1039/b906292k
- Lower, C. S., Cann, J. H., & Haynes, D. (2013). Microfossil Evidence for Salinity Events in the Holocene Coorong Lagoon, South Australia. *Australian Journal of Earth Sciences*, 60(5), 573-587. doi:10.1080/08120099.2013.823112
- McArthur, J. M., Howarth, R. J., & Bailey, T. R. (2001). Strontium Isotope Stratigraphy: Lowess Version 3: Best Fit to the Marine Sr-Isotope Curve for 0–509 Ma and Accompanying Look-up Table for Deriving Numerical Age. *The Journal of Geology*, 109(2), 155-170. doi:10.1086/319243
- McKirdy, D. M., Thorpe, C. S., Haynes, D. E., Grice, K., Krull, E. S., Halverson, G. P., & Webster, L. J. (2010). The Biogeochemical Evolution of the Coorong During the Mid- to Late Holocene: An Elemental, Isotopic and Biomarker Perspective. *Organic Geochemistry*, 41(2), 96-110. doi:10.1016/j.orggeochem.2009.07.010
- Mosley, L., Ye, Q., Shepherd, S., Hemming, S., & Fitzpatrick, R. (2018). *Natural History of the Coorong, Lower Lakes, and Murray Mouth Region (Yarluwar-Ruwe)*(pp. 522).
- Phillips, W., & Muller, K. (2006). Ecological Character of the Coorong, Lakes Alexandrina and Albert Wetland of International Importance., from South Australian Department of Environment and Heritage
- Phillis, C. C., Campana, S., Ostrach, D. J., Ingram, B. L., & Weber, P. K. (2011). Evaluating Otolith Sr/Ca as a Tool for Reconstructing Estuarine Habitat Use. *Canadian Journal of Fisheries and Aquatic Sciences*, 68(2), 360-373. doi:10.1139/f10-152
- Reeves, J. M., Haynes, D., García, A., & Gell, P. A. (2014). Hydrological Change in the Coorong Estuary, Australia, Past and Present: Evidence from Fossil Invertebrate and Algal Assemblages. *Estuaries and Coasts*, 38(6), 2101-2116. doi:10.1007/s12237-014-9920-4
- Saunders, K. M., McMinn, A., Roberts, D., Hodgson, D. A., & Heijnis, H. (2007). Recent Human-Induced Salinity Changes in Ramsar-Listed Orielton Lagoon, South-East Tasmania, Australia: A New Approach for Coastal Lagoon Conservation and Management. *Aquatic Conservation: Marine and Freshwater Ecosystems*, 17(1), 51-70. doi:10.1002/aqc.732

- SCHÖNE, B. D., ZHANG, Z., JACOB, D., GILLIKIN, D., TÜTKEN, T., GARBE-SCHÖNBERG, D., MCCONNAUGHEY, T., & SOLDATI, A. (2010). Effect of Organic Matrices on the Determination of the Trace Element Chemistry (Mg, Sr, Mg/Ca, Sr/Ca) of Aragonitic Bivalve Shells (*Arctica Islandica*) - Comparison of Icp-Oes and La-Icp-MS Data. *Geochemical Journal*, 44, 23 - 37. doi:10.2343/geochemj.1.0045
- SHALEV, N., GAVRIELI, I., HALICZ, L., SANDLER, A., STEIN, M., & LAZAR, B. (2017). Enrichment of ^{88}Sr in Continental Waters Due to Calcium Carbonate Precipitation. *Earth and Planetary Science Letters*, 459, 381-393. doi:10.1016/j.epsl.2016.11.042
- SHAO, Y., FARKAŠ, J., HOLMDEN, C., MOSLEY, L., KELL-DUIVESTEIN, I., IZZO, C., REIS-SANTOS, P., TYLER, J., TÖRBER, P., FRÝDA, J., TAYLOR, H., HAYNES, D., TIBBY, J., & GILLANDERS, B. M. (2018). Calcium and Strontium Isotope Systematics in the Lagoon-Estuarine Environments of South Australia: Implications for Water Source Mixing, Carbonate Fluxes and Fish Migration. *Geochimica et Cosmochimica Acta*, 239, 90-108. doi:10.1016/j.gca.2018.07.036
- SHAO, Y., FARKAŠ, J., MOSLEY, L., TYLER, J., WONG, H., SAMANTA, M. H., CHEN, G., GILLANDERS, B. M., KOLEVICA, A., & EISENHAEUER, A. (Submitted). *Impact of Salinity and Carbonate Saturation on Stable Sr Isotopes ($^{88}/^{86}\text{Sr}$) in a Lagoon-Estuarine System*. Submitted and under review in *Geochimica et Cosmochimica Acta*.
- SINGURINDY, O., BERKOWITZ, B., & LOWELL, R. P. (2004). Carbonate Dissolution and Precipitation in Coastal Environments: Laboratory Analysis and Theoretical Consideration. *Water Resources Research*, 40(4). doi:10.1029/2003wr002651
- TULIPANI, S., GRICE, K., KRULL, E., GREENWOOD, P., & REVILL, A. T. (2014). Salinity Variations in the Northern Coorong Lagoon, South Australia: Significant Changes in the Ecosystem Following Human Alteration to the Natural Water Regime. *Organic Geochemistry*, 75, 74-86. doi:10.1016/j.orggeochem.2014.04.013
- VOLLSTAEDT, H., EISENHAEUER, A., WALLMANN, K., BÖHM, F., FIETZKE, J., LIEBETRAU, V., KRABBENHÖFT, A., FARKAŠ, J., TOMAŠOVÝCH, A., RADDATZ, J., & VEIZER, J. (2014). The Phanerozoic $\Delta^{88}/^{86}\text{Sr}$ Record of Seawater: New Constraints on Past Changes in Oceanic Carbonate Fluxes. *Geochimica et Cosmochimica Acta*, 128, 249-265. doi:10.1016/j.gca.2013.10.006
- WEBER, M., LUGLI, F., JOCHUM, K. P., CIPRIANI, A., & SCHOLZ, D. (2018). Calcium Carbonate and Phosphate Reference Materials for Monitoring Bulk and Microanalytical Determination of Sr Isotopes. *Geostandards and Geoanalytical Research*, 42(1), 77-89. doi:10.1111/ggr.12191
- WEBSTER, I. T., & HARRIS, G. P. (2004). Anthropogenic Impacts on the Ecosystems of Coastal Lagoons: Modelling Fundamental Biogeochemical Processes and Management Implications. *Marine and Freshwater Research*, 55, 67-78. doi:10.1071/MF03068
- WELLS, F. E., & THRELFALL, T. J. (1982). Reproductive Strategies of *Hydrococcus Brazieri* (Tenison Woods, 1876) and *Arthritica Semen* (Menke, 1843) in Peel Inlet, Western Australia. *Journal of the Malacological Society of Australia*, 5(3-4), 157-166. doi:10.1080/00852988.1982.10673947





9 APPENDIX

9.1 Appendix A: Method

9.1.1 SHELL CLASSIFICATION

It is possible that the presence of periostracum could influence levels of certain trace elements (including Sr, Mg, etc) in acid digested bulk shells and therefore the interpretation of acquired concentration data. In this study, the temporal Sr concentration trend based on the analysis of fossil shells was constructed using 10-20 shells collected from an individual depth horizon within the core, so that there was a good representation of 'bulk shells' sample, each composed of several carbonate individuals. Colouration in carbonates can be loosely distinguished visually using a binocular microscope. Following the above reasoning, the redeposited shells might be characterised by a general lack in lustre and colour (i.e. periostracum have been removed) and such shells can be also smoother across the growth rings. In-situ carbonates, however, are expected to be better preserved with pinkish hue due to presence of original periostracum coatings and can also be ridged along growth rings (James & Bone, 2011). As there is not a definite distinction available for the studied species, this method should be used with caution and there should be a modern equivalent to compare fossil shells colouration for possible diagenetic coatings due to Fe and Mn oxyhydroxides and staining.

Table A 1. Examples of colour separation in both modern and fossil shells.

	Palaeo Core-1: 80cm (bottom of the core dated at 3275 years ago)	Modern Sample: Coor-50 (Tauwitchere)
White		
Pink		

Whilst there is a visible offset with no standard error overlap Table A1 in the stable strontium but overlap suggesting that they're not statistically different the data displayed in this thesis uses a sample size of 1 with no reproducibility because of the

time period that the sampling was conducted in. Increasing the sampling size would increase the confidence in how much of a isotopic difference the colour variants control.

9.1.2 RADIOGENIC $^{87}\text{Sr}/^{86}\text{Sr}$ AND STABLE $\Delta^{88/86}\text{Sr}$ ISOTOPES

The following methods contain relatively novel techniques developed in the last 10 years to improve accuracy and precision. In the case of $\delta^{88/86}\text{Sr}$ this is carried out by combining standards, sample spiking and iterative calculations to reduce the effect of preferential isotope fractionation causing isotopic variation. In the case of $^{87}\text{Sr}/^{86}\text{Sr}$ accuracy and precision are improved through improving machine error that can be caused by faraday cup degradation within the TIMS (Fukai et al., 2017). To purify from sample matrix prior to Sr isotope analysis on TIMS, all samples had to be processed via column chemistry or chromatography. Briefly, the Sr SPS Micro Bin Spin column procedure was followed in this study to appropriately clean column and resin and collect sample or pure Sr fractions. Double spiked (DS) and un-spiked (further method in Appendix A) containers and Teflon vials were kept separated from each other during processing to avoid cross contamination from isotopically enriched double-spike (including whilst evaporating samples in the fume cupboard and the loading of the spike into the sample aliquots). Typical column chemistry procedural blanks were all below 0.1% of total Sr loaded and processed.

9.1.2.1 Preparation of sample and sample loading on rhenium filaments

Centre rhenium filaments used for Sr isotope analysis on TIMS were pre cleaned by submerging them in hydrogen peroxide at 80°C for 1 hour, washing with DI water three times and then submerging in acetone and placing them in a sonic bath for 1 minute.

Such pre-cleaned filaments were placed in an oven overnight at 110°C, once dry the new rhenium filaments were then spot welded onto the clean posts for TIMS with the following procedure. Once welded, all filaments were placed in an Isotopx DG60 unit to degas overnight 110-240V for further cleaning via outgassing which was done under vacuum. Samples were loaded with the following procedure:

1. Load 1uL H₃PO₄ and evaporate at ~0.5A
2. Load 0.05uL Birks solution and dry at ~0.5A
3. Load ~500ng of Sr in ~uL Birks solution, dry at ~0.5A
4. Increase to ~1A observing load and reducing current if the sample moves towards the either post, over ~1 minute increase to ~1.8A and leave for 1 minute
5. Increase current to 2.3A or until cherry red and hold there for 3-5 seconds
6. Load filaments on TIMS turret according to bracketing procedure (see Table A2 below)

9.1.2.2 Double-spike method and standards

To improve accuracy and precision of measuring isotope ratio concentrations a method has been developed by Krabbenhöft et al. (2009) using a spike with a known ratio of two different strontium isotopes, this method is known as a double-spike (DS) as the solution contains a known ratio of two isotopes of Sr. The ratio within the DS is 48% solution containing ⁸⁷Sr and 52% solution containing ⁸⁴Sr (Krabbenhöft et al., 2009). A known amount of sample mixed with a known amount of double-spiked solution (DS3) for δ^{88/86}Sr analysis, but for ⁸⁷Sr/⁸⁶Sr analysis an un-spiked aliquot is used and measured via TIMS. The sample aliquots were then placed on a hotplate at 140°C and evaporated. Once the sample was fully evaporated, 1ml of 8M HNO₃ acid was added to

vials and the aliquot was capped to reflux for 2 hours the sample-spike solution. Instead of normalising Sr isotopic ratios solely to relevant standards such as seen in Table 1, a known concentration of $^{87/84}\text{Sr}$ is used together with these same standards. Each sample and standard containing the same amount of total Sr (500ng) that is measured though TIMS has a corresponding spiked partner with a known number of $^{87/84}\text{Sr}$ DS. This process accounts for ^{87}Sr to preferentially fractionating and causing the radiogenic $^{87}\text{Sr}/^{86}\text{Sr}$ ratio to have a greater variation in the results (Krabbenhöft et al., 2010). The Sr isotope results from standards, including IAPSO seawater and JcP-1 carbonate, are listed in Table 1; all standards were processed through column chemistry and TIMS and were also double spiked with DS3 and bracketed as seen in Table x. For optimal spiking conditions, the ‘sample to spike’ ratio of samples (also expressed as $84\text{Sr}_{\text{sp}}/84\text{Sr}_{\text{sa}}$ ratio) should be around 20 for all samples (Krabbenhöft et al., 2009).

Table A 2. Bracketing method used for loading centre filaments into the TIMS machine with the most optimal turret positions to calculate within session drift (Fietzke & Eisenhauer, 2006; Shao et al., 2018).

Turret Position	Sample	Use
1	Blank	Measure lab conditions
2	987 (TIMS solution)	TIMS lab condition blanks
3	NIST SRM 987a	Long and short term SRM averages
4	NIST SRM 987a DS	
5	Sample a	Site samples
6	Sample a DS	
7	Sample b	
8	Sample b DS	
9	Sample c	
10	Sample c DS	
11	JcP-1 or IAPSO	Shell or seawater known value
12	JcP-1 or IAPSO DS	

13	Sample d	
14	Sample d DS	Site Samples
15	Sample e	
16	Sample e DS	
17	987 (TIMS solution)	
18	NIST SRM 987b	Long and short term SRM averages
19	NIST SRM 987b DS	
20	Sr + Rb	Calculate naturally occurring ^{87}Rb and ^{87}Sr

9.1.2.3 Dynamic vs static

Higher amounts of precision are achieved when observing $^{87}\text{Sr}/^{86}\text{Sr}$ using a dynamic method through the TIMS as this negates potential Faraday cup degradation issues. It has been observed that high-use of TIMS machines can result in inaccurate readings from degradation and also sample build up on the Faraday cups (Fukai et al., 2017). This dynamic method increases precision through cycling the Faraday cups and normalising readings across all cups. A single $^{87}\text{Sr}/^{86}\text{Sr}$ value is given from multiple measurements to decrease potential uncertainty from Faraday cup degradation (Fukai et al., 2017). Dynamic measurements were used for $^{87}\text{Sr}/^{86}\text{Sr}$ ratios to account for faraday cup degradation (Fukai et al., 2017) and attain high precision of measured Sr isotope data. Static measurements are taken for the $\delta^{88/86}\text{Sr}$ in combination with the iterative DS calculation method carried out by Krabbenhöft et al. (2009) and Shao et al. (submitted). This involved comparing both DS and un-spiked samples through five iterations of normalizing calculations comparing the known amount of $^{87}\text{Sr}/^{86}\text{Sr}$ ratio found in the DS to the known total strontium amount (500ng) in each sample.

9.2 Appendix B: ICP-MS

Appendix B1 shows a strong linear relationship with an r^2 value of higher than 0.999, this displays certainty in the data output from any potential systematic errors that could influence elemental concentration output.

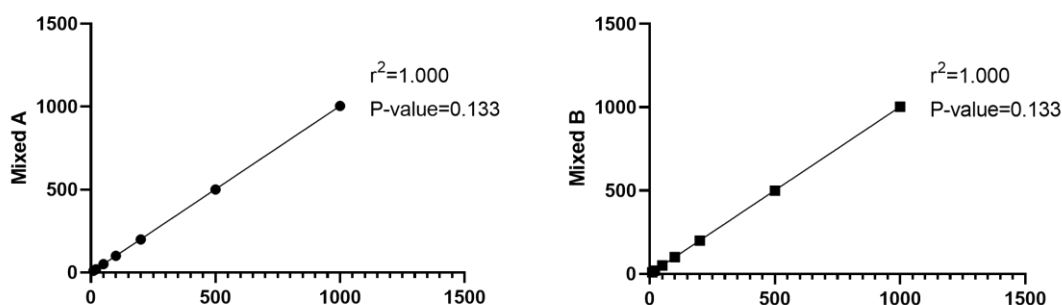


Figure B 3. ICP calibration curve for known elemental concentrations in standard solutions Mixed A and Mixed B

Table B 1 Elemental concentration in parts per billion (ppb) of modern waters sampled in 2020 with corresponding % relative standard deviation (%RSD) and partial salinity units (PSU).

Sample month	Sample	Salinity (PSU)	Sr (ppb)	%RSD	Mg (ppb)	%RSD
February	LZ1	99	402.9782	0.202326	60237.11	1.265197
	LZ3	99.34	243.2784	8.535479	36781.27	0.430311
	LZ5	99.21	221.7619	2.771326	37961.56	1.494862
March	COOR-01	103.88	238.6152	2.511895	41366.24	2.667077
	COOR-07	106.21	217.4273	1.084087	37055.53	0.881395
	COOR-04	106.41	495.5096	1.71766	75176.77	1.949007
	COOR-50	31.5	247.0105	1.095423	41713.31	1.09817
	SCR	14.95	538.3037	1.732028	33684.54	1.670308
July	N5	83.16	219.876	0.090121	36067.8	0.939244
	S7	84.25	237.8506	1.233457	35060.93	1.757116
	S6	84.25	322.631	3.037996	46190.72	0.717751
	N9	29.42	165.4489	1.865642	27173.12	0.938525
	SCR(2)	9.99	583.5217	1.270173	34174.11	1.481371

Table B 2. Elemental concentration in parts per billion (ppb) of modern shells sampled in March 2020 with corresponding core depth and % relative standard deviation (%RSD). Sediment at 80cm is carbon dated at 3275 B.P.

Relative age	Depth (cm)	Sr (ppb)	%RSD	Mg (ppb)	%RSD
Modern	0	137.4934	2.167475	15.34878	0.747539
	0	134.1354	0.838803	14.68883	0.239266
	2	365.5557	0.317318	37.88047	0.490985
	6	296.3012	1.415392	20.28548	3.049102
	10	303.8224	2.912189	24.65011	1.771623
	14	353.8683	1.161458	24.15697	2.39755
	18	347.545	9.430028	20.49252	0.775976
	25	319.2928	0.829039	21.8057	0.757503
Fossil	30	270.9294	6.124245	18.33227	2.423454
	40	255.895	1.167529	18.67251	1.815683
	50	308.4075	0.721603	21.47239	1.643825
	55	277.6825	2.254169	23.82439	1.627617
	65	294.8794	2.257337	22.62097	4.219684
	70	246.2192	1.008591	18.95703	5.329401
	80	223.3737	0.562266	21.89673	2.007007
	80	152.0104	1.36278	13.73652	1.484965

9.3 Appendix C: TIMS

Table C 1. Individual and averaged SRM 987 values in comparison with JCP and IAPSO standards. Grey highlighted values were used in standard and sample iterative processing.

Magazine	Isotope Ratios of SRM 987				$\delta^{88}\text{Sr}$ ‰	IAPSO standard		
	86/84Sr	88/84Sr	87/84Sr	88/86Sr		2*SE	Reason for omitting	
Run 1	SRM 987 a	17.5263	145.401	12.38873	8.29618	0.388	0.012	
	SRM 987 b	17.5296	145.430	12.39076	8.29625	0.380	0.012	
	Average	17.5279	145.416	12.38974	8.29622	0.384	0.012	
Run 2	SRM 987 a	17.5286	145.436	12.39065	8.29706	0.408	0.013	
	SRM 987 b	17.5327	145.508	12.39405	8.29925	0.144	0.013	C-Chart diagnostic unfit
	Average	17.5306	145.472	12.39235	8.29816	0.276	0.013	987 b skewed average
Run 3	SRM 987 a	17.5277	145.421	12.38989	8.29661	0.363	0.012	
	SRM 987 b	17.5272	145.420	12.38907	8.29682	0.338	0.012	Unfit IAPSO standard
	Average	17.5275	145.421	12.38948	8.29672	0.350	0.012	987b skewed average
Run 4	Isotope Ratios of SRM 987				JCP-1 standard			
	SRM 987 a	17.5278	145.413	12.38926	8.29612	0.285	0.013	unfit JCP standard
	SRM 987 b	17.5287	145.430	12.39029	8.29664	0.223	0.013	
	Average	17.5283	145.421	12.38977	8.29638	0.254	0.013	987 a skewed average
Run 5	SRM 987 a	17.5274	145.414	12.38907	8.29641	0.223	0.012	
	SRM 987 b	17.5262	145.410	12.38800	8.29671	0.188	0.012	unfit JCP standard
	Average	17.5268	145.412	12.38853	8.29656	0.127	0.012	987 b skewed average
Run 6	SRM 987 a	17.5274	145.414	12.38907	8.29641	0.230	0.014	
	SRM 987 b	17.5262	145.410	12.38800	8.29671	0.195	0.014	
	Average	17.5268	145.412	12.38853	8.29656	0.212	0.014	

Table C 2. Amount of sample loaded on to the TIMS for 500ng of strontium in modern waters using total known Sr concentration from ICP-MS and calculated dilution factors (DF). The highlighted numbers were used in the actual analysis of the samples because of uncertainty in ICP results.

Date	Sample	Salinity (PSU)	Sr Concentration in ICP solution (ppb)	Calculated DF 1	stock solution for 500 ng of Sr (ml)	Calculated 500ng of Sr using Equation 1 (ml)
February 2020	LZ1	99	402.98	92.76	0.0134	0.0220
	LZ3	99.34	243.28	54.21	0.0379	0.0219
	LZ5	99.21	221.76	49.99	0.0046	0.0219
March 2020	COOR 01	103.88	238.62	93.02	0.0225	0.0210
	COOR 04	106.21	217.43	80.84	0.0220	0.0205
	COOR 07	106.41	495.51	104.35	0.0125	0.0205
	COOR 50	31.5	247.01	28.98	0.0698	0.0662
	SCR	14.95	538.30	14.86	0.0625	0.1307
July 2020	N5	29.42	219.88	29.15	0.0780	0.0706
	S7	84.25	237.85	111.12	0.0189	0.0257
	S6	84.25	322.63	95.24	0.0163	0.0257
	N9	83.16	165.45	96.48	0.0313	0.0261
	SCR(2)	9.99	583.52	9.92	0.0863	0.1846

Table C 3. Amount of sample loaded on to the TIMS for 500ng of strontium in modern and fossil carbonates using total known Sr concentration from ICP-MS and calculated dilution factors.

	Sample	Sr Concentration in ICP solution (ppb)	Calculated DF 2 Amount given to ICP (g)/Weighed sample solution (g)	Concentration in stock solution Sr Conc in ICP solution*calculated DF 2	500ng of Sr (ml stock solution) 500/concentration in stock solution
Modern	COOR-50-P	137.49	9.99	1373.07	0.36
	COOR-50-W	134.14	9.96	1335.99	0.37
	core-02-P	365.56	10.08	3686.19	0.14
	core-06-P	296.30	9.90	2933.53	0.17
	core-10-P	303.82	10.22	3104.60	0.16
	core-14-P	353.87	9.90	3502.00	0.14
	core-18-P	347.54	10.00	3474.89	0.14
	core-25-P	319.29	10.07	3215.25	0.16
	core-30-P	270.93	10.03	2718.07	0.18
	core-40-P	255.90	10.02	2563.15	0.20
	core-50-P	308.41	9.97	3074.26	0.16
	core-55-P	277.68	10.00	2777.05	0.18
	core-65-P	294.88	9.91	2922.61	0.17
	core-70-P	246.22	10.01	2465.55	0.20
Fossil	core-80-P	223.37	9.96	2225.00	0.22
	core-80-P	152.01	9.99	1518.06	0.33
	core-80-W	137.49	9.99	1373.07	0.36

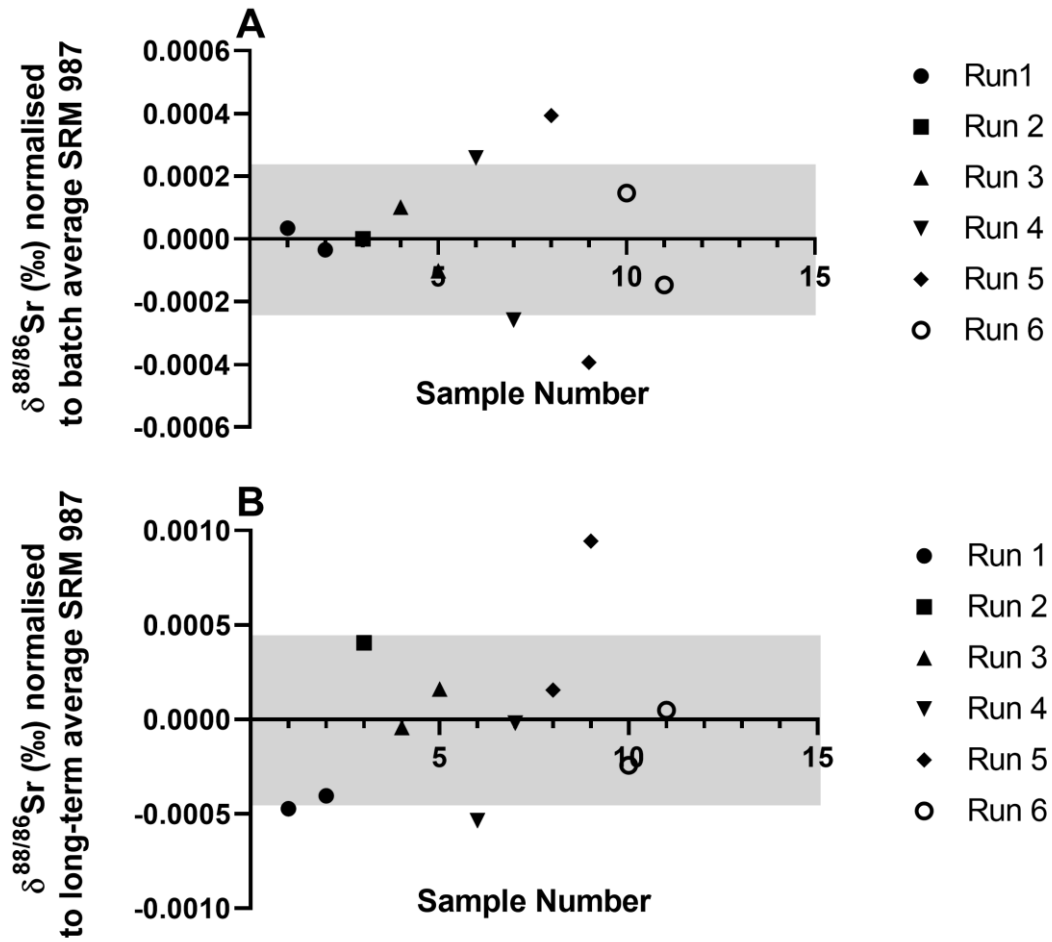


Figure C 1. (A) Normalised $\delta^{88/86}\text{Sr}$ to all batch averages representing within session drift with a SD of $\pm 0.00022\text{‰}$ and (B) normalised $\delta^{88/86}\text{Sr}$ to long term (February 2020 to July 2020) between session drift for the NIST SRM 987 run through TIMS dynamic and static measurements with a SD of $\pm 0.0004\text{‰}$. Black solid line is the mean and the grey box is 2SD (2 standard deviation).